ELSEVIER

Contents lists available at ScienceDirect

Science of the Total Environment

journal homepage: www.elsevier.com/locate/scitotenv



Check for updates

Legacy of severe soil degradation hinders the buildup of mineral-associated soil organic carbon

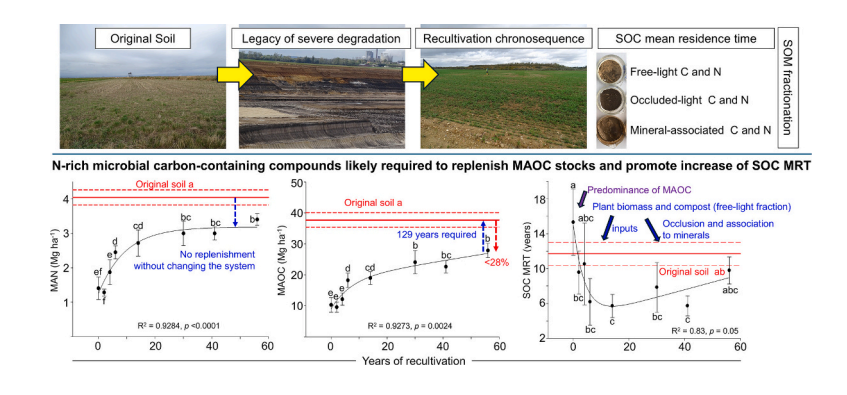
Otávio dos Anjos Leal*, Rüdiger Reichel, Holger Wissel, Nicolas Brüggemann

Institute of Bio- and Geosciences—Agrosphere (IBG-3), Forschungszentrum Jülich GmbH, Wil-helm-Johnen-Straße, 52428 Jülich, Germany

HIGHLIGHTS

- 56-year conventional agriculture chronosequence unravelling SOC accrual constraints.
- 93 and 129 years are estimated to replenish total and mineral-associated SOC stocks.
- MAN stocks stagnation indicates Ndeficit for microbial-derived C stabilization.
- MAOC accrual limited by N and system, rather than by minerals C-saturation.
- Optimization of C and mainly N needed to achieve higher MAOC and SOC steady-states.

GRAPHICAL ABSTRACT



ARTICLE INFO

Editor: Wei Shi

Keywords:
Agricultural chronosequence
Density fractions
Nitrogen
Carbon mean residence time
Steady-state
Non-saturation
PCA

ABSTRACT

Global efforts target a soil organic carbon (SOC) enhancement rate of 2.4 ‰ y⁻¹ in the upper 30 cm of agricultural soils to address declining soil productivity associated with declining SOC stocks. We explored a unique chronosequence of homogeneous soils formed after mining in Germany, which serve conventional agriculture and exhibit a large margin for SOC storage, but limited SOC accrual, to study SOC protection mechanisms and accrual constraints. We hypothesized that limited SOC accrual is associated to insufficient nitrogen rather than to minerals saturation. Soil samples (0-30 and 30-60 cm) were collected across the chronosequence (0-56 years) and compared to an original non-mined soil (OS) managed similarly. The mean residence time (MRT) of SOC and its protection mechanisms were studied using soil incubation, organic matter density fractionation, and δ^{13} C measurements. After 56 years, total and mineral-associated SOC (MAOC) stocks remained 18 % and 28 % lower than in the OS at 0-30 cm, with estimated replenishment times of 93 and 129 years, respectively. Mineralassociated nitrogen (MAN) stocks stagnated along recultivation time below OS level. Together with significant linear correlation of MAOC with total SOC and MAN stocks, these results indicate that nitrogen rather than saturation of minerals limits SOC accrual. In fact, the MAOC stock deficit to saturation was estimated at 316.4 Mg ha⁻¹. At 30–60 cm, SOC and nitrogen stocks were restored within 30 years, due to comparatively lower initial losses. The initial MRT of SOC at 0-30 and 30-60 cm (15.3 and 27.9 years) declined before finally becoming comparable to OS (11.7 and 7.7 years). This reflected new carbon entering the soil that initially contained predominantly MAOC (78-82 %), followed by its stabilization as MAOC. Due to their susceptibility to nitrogen

E-mail address: o.dos.anjos.leal@fz-juelich.de (O.A. Leal).

^{*} Corresponding author.

1. Introduction

Soils are the largest terrestrial reservoir of organic carbon (C), storing approximately 793, 1502 and 1993 Pg C to a depth of 30, 100 and 200 cm, respectively (Jobbágy and Jackson, 2000; Padarian et al., 2022). The estimated loss of soil organic C (SOC) due to agricultural land use for the top 30, 100 and 200 cm of soil is 37, 75 and 133 Pg C, respectively (Sandermann et al., 2017). Between 2001 and 2020, the estimated global average loss of SOC from the 0–30 cm layer was 1.9 Pg C y^{-1} (2.4 % y^{-1}), strongly driven by agriculture intensification, soil erosion and accelerated SOC mineralization rates, resulting in increased atmospheric CO₂ concentrations and decreased soil productivity (Padarian et al., 2022).

Globally, >33% of soils are already moderately or severely degraded (FAO, 2022). Each year, 11.07 and 5.36 million hectares in the tropical and temperate regions of the world fall below the critical SOC thresholds for soil productivity (estimated as 1.1 and 2% SOC at 0-30 cm layer for tropical and temperate regions, respectively) due to intensive agricultural production practices (Padarian et al., 2022). It is generally agreed that SOC accounts for 58 % of soil organic matter (SOM) (Stockmann et al., 2013), which improves multiple soil attributes, such as nutrient and water retention capacity, thereby increasing crop yields and soil resilience to adverse climate (Schmidt et al., 2011; Machmuller et al., 2015; Tian et al., 2024). Furthermore, a minimum SOC enhancement rate of 2.4 % y^{-1} (equivalent to 4 % y^{-1} SOM) in the 0–30 cm layer of agricultural soils has been targeted to regulate atmospheric CO₂ concentration and to combat food insecurity (Padarian et al., 2022).

Soils with higher silt and clay content combined with low SOC stocks are of particular interest for SOC accrual due to the available and highly interactive mineral surfaces (Kleber et al., 2015; Lugato et al., 2021), which promote long-term SOC stabilization (Haddix et al., 2020; Mao et al., 2024). Long-term SOC persistence is strongly influenced by physical barriers between microbial decomposers and the organic material (e.g., SOC occlusion in aggregates) and organo-mineral interactions that inhibit SOC decomposition by microorganisms (Cotrufo and Lavalle, 2022). These SOC protection mechanisms can be studied by SOM density fractionation. This method typically separates SOM in free fractions: the free light fraction (FLF) refers to SOC lacking significant protection by aggregation or association with minerals, but not physically disconnected from microbes and their enzymes; the occluded light fraction (OLF) refers to SOC protected by physical occlusion in aggregates, which limits O2 diffusion and accessibility of microorganisms and enzymes to the C source; and the heavy fraction (HF) refers to SOC intimately bound to soil minerals, thereby limiting microbial and enzymatic access to the C substrate (Plaza et al., 2019). Such SOM fractionation methods, together with nitrogen (N) fractionation, have been proposed as a means of identifying constraints in SOC storage in agricultural soils (Hansen et al., 2024).

Mineral-associated SOM has been shown to consist largely of N-rich microbial products, whereas particulate SOM consists primarily of plant residues, with a predominance of structural C and a low N content (Cotrufo et al., 2019). Thus, mineral-associated SOM has lower turnover rates but requires greater N input (e.g., N-rich crop residues) for its formation compared to particulate SOM (Manzoni and Cotrufo, 2024). Labile SOM may be readily biodegraded, yet it stimulates the formation of aggregates and SOC occlusion and is a precursor of mineral-associated SOC (Angst et al., 2023), which has a longer mean residence time (MRT) (Paul et al., 2008). The MRT of SOC is recognized as an indicator of the relative efficiency of SOC sequestration under specific soil, climate, or management conditions (Poeplau et al., 2021).

Globally, the mineral-associated SOC stock of non-permafrost

mineral soils is estimated to be 899 Pg down to 1 m depth (Georgiou et al., 2022). Mineral-associated SOC represents 66 and 70 % of the total SOC in the 0–30 and 30–100 cm soil layers, respectively, but this represents only 42 and 21 % of the mineralogical capacity of these layers for SOC storage, with larger deficits reported for agricultural soils and subsurface layers (Georgiou et al., 2022). Moreover, SOC can further accumulate in SOC-saturated mineral surfaces by association with organic compounds bound to the minerals (Begill et al., 2023). Therefore, large-scale SOC stabilization in fine-textured agricultural soils is an important solution to accelerate SOC sequestration (Manzoni and Cotrufo, 2024).

Recultivation and restoration of SOC stocks of severely degraded soils is particularly urgent in the context of international initiatives to ensure global food security and combat climate change (European Commission, 2021). However, the temporal evolution of SOC protection mechanisms and MRT in soils recultivated after severe degradation is poorly understood and requires appropriate model sites to be studied. Filling this knowledge gap is urgently needed to reveal constraints on SOC accrual and to redirect recultivation practices towards strategic SOC stabilization.

In North Rhine-Westphalia (NRW), Germany, >250,000 ha of marginal soils have been created by open-cast lignite mining activities in the last 50 years (Reichel et al., 2024). This is considered the largest cohesive lignite seam in Europe (Maaßen and Schiffer, 2019). Continuous mining followed by standardized soil profile reconstruction and recultivation procedures (Lössabkommen, 1961; Landesoberbergamt, 1986; Dworschak and Rose, 2014) in this region have created a chronosequence of soils with homogeneous texture and SOC content. These soils are mostly used for the conventional farming of wheat, barley, sugar beet, potato and canola, with highly comparable practices across fields. Thus, this chronosequence can be reliably used as a model site to reveal constraints on SOC accrual as well as the evolution of basic SOC protection mechanisms with increasing agricultural age, here from 0 to 56 years. These soils have 17 % clay and 78 % silt, and a low initial total N content <1 g kg⁻¹ and an SOC content <4 g kg⁻¹. The availability of an adjacent original soil (OS, Luvisol) with similar texture and agricultural history serves as optimal reference.

In this chronosequence, the SOC stock deficits in the 0–30 cm soil layer after 0 and 62 years of recultivation were 39.1 and 20.7 Mg C ha $^{-1}$, respectively, compared to the average SOC stock of croplands in German Luvisols (Poeplau et al., 2020; Zhao et al., 2022). The extent of these deficits below 30 cm remains unknown, as does the stability of the new SOC stocks along the soil profile. The rates of SOC accrual in the 0–30 cm layer of these soils decreased from 1.50 Mg C ha $^{-1}$ y $^{-1}$ after 7 years to 0.30 Mg C ha $^{-1}$ y $^{-1}$ after 62 years of recultivation, when the total SOC stock was 26.7 Mg C ha $^{-1}$ (Zhao et al., 2022). These SOC accrual rates and SOC stocks were 63–93 % and 55 % lower, respectively, compared to that of a soil of similar location, initial SOC stock and coarser texture but recultivated with *Robinia pseudoacacia* L. for 14 years (Matos et al., 2012). Altogether, these contrasting results suggest that SOC accrual in soils under agricultural recultivation is likely limited by the cultivation system rather than by soil texture.

In this study, we aimed to: i) determine occluded and mineral-associated SOC stocks over time, both within and below the plough layer, following the implementation of conventional agriculture in severely degraded soils; ii) analyze how the MRT of SOC changes during recultivation; and iii) explore the potential to optimize these fine-textured soils for long-term SOC storage. We hypothesized that: i) the declining rates of SOC accrual during recultivation are mainly caused by declining rates of mineral-associated SOC accrual; ii) the limited accrual of mineral-associated SOC is accompanied by limited accrual of mineral-

associated N; iii) the accrual of mineral-associated SOC is limited by the recultivation system rather than by the mineralogical capacity of the soil.

2. Materials and methods

2.1. Study site and chronosequence of minesoils: formation and recultivation

The study area is situated near Inden in North-Rhine Westphalia, western Germany. The region experiences an average annual air temperature of 9.8 °C and an average annual precipitation of 829 mm (Deutscher Wetterdienst, https://www.dwd.de). The mean elevation is 122 m above sea level. The non-mined original soil (OS) is classified as Luvisol (IUSS Working Group WRB, 2015).

The chronosequence of minesoils is established after open-cast lignite mining through a three-step process: 1) excavation: the mining company (RWE Power AG, Essen, Germany) removes the original soil loess layer and underlying tertiary sands (>100 m deep) to access the lignite deposits. This is achieved though stratified digging; 2) backfilling: the removed soil loess and sandy substrates are transported via large conveyor belts from the excavation front to the backside of the mine, where mining operations are concluded, to fill the cavity left by lignite extraction. The sandy substrate is deposited first, followed by the formation of a 2 m soil profile by evenly homogenized soil loess material on top; 3) recultivation: recultivation is carried out in three phases. Recultivation phase 1 (RP1): continuous alfalfa cultivation is implemented for three years with fertilization (60 kg ha⁻¹ N, 120 kg ha⁻¹ P, and 180 kg ha⁻¹ K) applied only in the first year. No biocide treatments or tilling are performed. At the end of the third year of alfalfa, compost (30-40 Mg ha⁻¹) is applied to soil, which is subsequently tilled, characterizing the end of RP1. Recultivation phase 2 (RP2): four-year cropping cycle of winter wheat, winter barley, canola and sugar beet is initiated. In the first and fourth years, cereals are supplemented with 30-40 Mg ha⁻¹ of compost in addition to mineral fertilizers (NPK and calcium ammonium nitrate). Total annual fertilization includes 200 kg ha^{-1} N, 80 kg ha^{-1} P, 60 kg ha^{-1} K, and 40 kg ha^{-1} Mg. Both RP1 and

RP2 are managed by RWE. Recultivation phase 3 (RP3): the land is transferred to farmers who implement conventional agriculture, typically involving the same crops mentioned in RP2. Complementary details about formation and recultivation of the chronosequence of minesoils can be found in Schmid et al. (2020) and Roy et al. (2023).

Since 1957, the processes of mining and recultivation have been carried out concurrently and continuously, creating a chronosequence of soils with comparable parent material but varying recultivation ages (belonging to RP1, RP2, or RP3). The recultivated soils typically contain 70–80 % silt, 10–22 % clay, and 2–9 % sand, and exhibit a silt loam texture according to the IUSS Working Group WRB (2015). The OS exhibits a similar texture (Schmid et al., 2020), pH between 6.5 and 7.0 (0–60 cm layer), SOC content <1.5 % at 0–30 cm and <1.0 % at 30–60 cm layer, and total N content <0.13 % at 0–30 cm and <0.10 % at 30–60 cm layer.

2.2. Soil sampling

Soil samples were collected from eight sites spanning a 56-year recultivation chronosequence (Fig. 1). Minesoils with 0, 2, 4, 6, 14, 30, 41 and 56 years of recultivation were sampled. For reference, samples were also taken from an OS (Luvisol) with a long history of agricultural use consisting of practices and crops comparable to that of the chronosequence of the recultivated soils. The OS was situated in the excavation front and represented the pre-mining conditions.

At the time of sampling, the soil with 0 and 2 years of recultivation were in RP1; the soil with 4 years of recultivation was at the end of RP1; the soil with 6 years of recultivation was in RP2; and the soils with 14, 30, 41 and 56 years of recultivation were in RP3. For each site, five minimally disturbed and three undisturbed soil samples were collected from two layers: 0–30 cm (plough) and 30–60 cm (below-plough) layer. The minimally disturbed soil samples (approximately 1 kg per replicate) were collected using a shovel. In the laboratory, soil aggregates were carefully broken manually along the natural planes of weakness, airdried, and passed through an 8-mm sieve. The mass of soil retained on the 8-mm sieve and that passing through a 2-mm sieve was recorded. The undisturbed soil samples were collected using steel cylinders

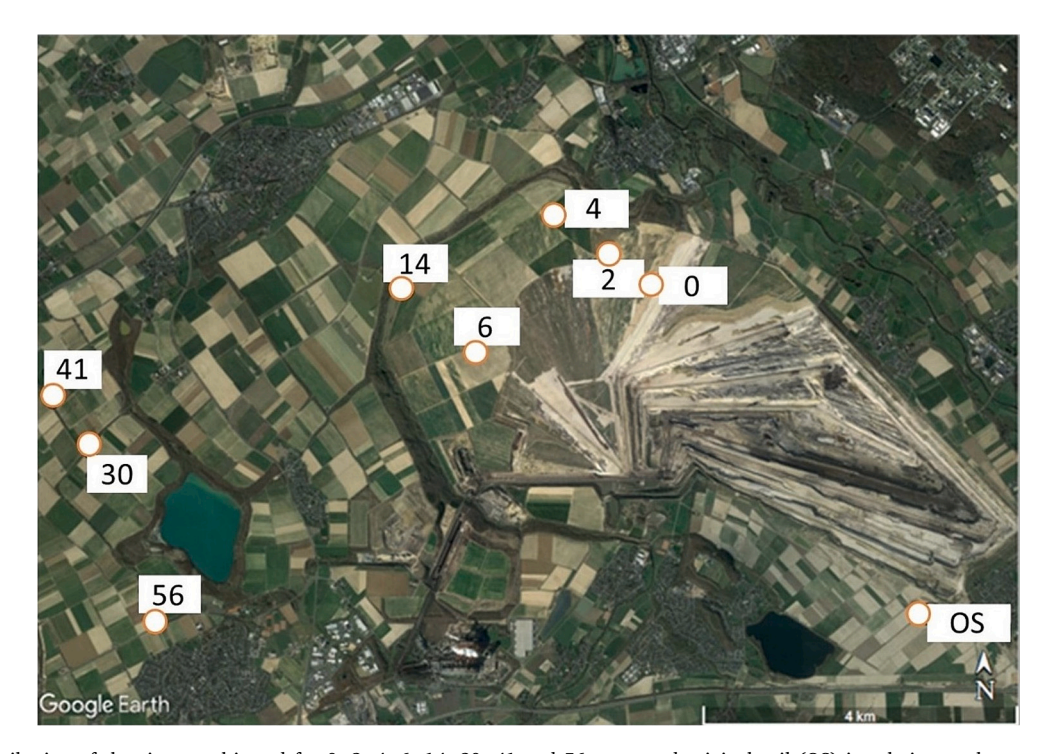


Fig. 1. Spatial distribution of the sites recultivated for 0, 2, 4, 6, 14, 30, 41 and 56 years and original soil (OS) in relation to the open-cast lignite mine in Inden, Germany.

(internal diameter 5.59 cm and height 4.06 cm) to determine soil bulk density (BD). To ensure spatial independence, each sampling point was located at least 12 m from the nearest sampling point within the field (sampling point coordinates are provided in Table S1).

One composite soil sample, consisting of soil from the five sampling

derived from the relation between CO_2 flux and measurement time exhibited $R^2 > 0.81$, and therefore were assumed as significant. The CO_2 flux derived from SOC (mg CO_2 -OC m^{-2} day $^{-1}$) was obtained according to Eq. (1):

$$F\left(\text{mg CO}_2 - \text{OC m}^{-2} \text{ day}^{-1}\right) = \left(\left(\frac{S}{1000000} \times \frac{P}{R \text{ T}} \times \frac{V}{A} \times \text{M} \times 60 \right) - \text{ICCO}_2\right) \times 24 \tag{1}$$

points within each field, was collected and stored for the preparation of a microbial solution for the incubation experiment (see details in Section 2.4).

2.3. Soil physical and chemical parameters

Soil moisture was determined gravimetrically. Soil water holding capacity (WHC) was measured according to Öhlinger (1996) using 30 g of air-dried 2 mm-sieved soil samples. The mass of dry soil into the steel cylinder divided by the volume of the cylinder represented the soil BD. Soil pH was measured using a multi 340i pH-meter (WTW GmbH, Germany) after mixing air-dried 2-mm sieved soil samples with 0.01 M calcium chloride (1:2.5, w/v), according to VDLUFA (1991). The soil pH, BD and WHC data are displayed in Table S2.

2.4. Incubation experiment for estimation of the MRT of SOC

PVC tubes (21.5 cm height, 4.5 cm internal diameter) with sealed bottom were filled with 250 g of air-dried 2-mm sieved soil samples to a BD of approximately 1.5 g cm⁻³ (as field BD, Table S2). Composite soil samples collected from each site and soil layer were kept frozen until preparation of microbial solutions. To prepare the inoculum, these samples were incubated for six days at 25 °C and 60 % WHC. Thereafter, 5 g of soil was shaken with 50 mL of distilled water for 1 h, then filtered (5 μm pore size) to recover the inoculum as similarly performed in Crow et al. (2006), Creamer et al. (2013) and Knicker et al. (2013). Each inoculum was added to the corresponding incubation tube to establish microbial communities consistent with the different stages of soil recultivation (Roy et al., 2017, 2023; Schmid et al., 2020). The weight of the whole tube was recorded, and soil was kept at 60 % WHC by dripping deionized water on the soil surface with an automatic pipette. This was done at least once a week and at least 24 h before CO2 measurements throughout the experiment duration. The tubes were randomly placed in an incubation cabinet set to a temperature of 12 °C.

2.4.1. Soil CO2 flux measurements

For soil CO2 flux measurements, a PVC chamber lid (4.5 cm inner diameter, 10.6 cm height) with a rubber seal was securely attached to the incubation tubes to ensure a gas-tight seal. Soil CO2 flux was measured at a second-by-second resolution over a 7-min period using an infrared gas analyzer (G2508, Picarro, Inc., Santa Clara, CA, USA). Between measurements, a 2-min interval was awaited. The data from the first and last minute of each measurement were discarded to account for eventual fluctuations caused by pressure disturbance during the attachment and detachment of the chamber and the incubation tube. The chamber lid was equipped with two 1/4-inch ports, allowing 2.4 m long tubing to connect the chamber to the gas analyzer in a closed-loop system. To prevent pressure disturbance during measurement, a vent tube (1 m long) was installed through a third gas-tight stainless steel tube fitting (1/4 in) on the chamber lid. The chamber's empty space (0.359 L) together with the empty space of the incubation tube created a headspace ranging from 0.00042 to 0.00045 m³ depending on the soil BD achieved into the tube. Throughout the experiment, all the slopes where, F = flux of CO₂ derived from organic C; S = slope of the linear equation fitted to the total CO₂ detected into the chamber headspace over time of chamber deployment (ppm min⁻¹); 1,000,000 converts ppm (μ L L⁻¹) to L L⁻¹; P = air pressure (atm) at 80 m above sea level; R = universal ideal gas constant (m³ atm mol⁻¹ K⁻¹); T = average temperature (K) of the chamber during the deployment time; M = C molar mass (g mol⁻¹); 60 converts min to hours; ICCO₂ refers to CO₂ flux derived from inorganic C (mg m⁻² h⁻¹) estimated for the 0–30 and 30–60 cm soil layer; and 24 coverts hourly to daily flux.

After a three-day pre-incubation period, soil CO₂ flux measurements were taken on days 0, 2, 7, 15, 21, 28, 35, 49, 63, 77, 91, 105, 121, 135, 149, 163, 177, 191, 205, 219 and 233 of incubation. Cumulative CO₂ emissions were obtained by averaging the emissions of two consecutive days of measurement and multiplying it by the number of days between the measurements (Castro-Herrera et al., 2023). These partial cumulative CO2 data were summed to determine the total cumulative CO2 emissions, expressed as g of CO₂-C m⁻². All emitted CO₂-C was attributed to SOC loss after accounting for CO2 emissions from soil inorganic C (SIC). For that, a constant rate of SIC loss for the 0–30 cm (0.72 Mg ha⁻¹ y^{-1}) and 30–60 cm layer (0.55 Mg ha⁻¹ y^{-1}) was calculated from the negative linear relationship between SIC stock and year of recultivation $(0-30 \text{ cm}; R^2 = 0.87; 30-60 \text{ cm}; R^2 = 0.84, \text{ Fig. S1})$. These rates were adjusted to the soil layer into the incubation tube (15 cm), resulting in the following rates of SIC loss as CO₂: 15.1 and 11.4 mg m⁻² h⁻¹ for soil samples collected at 0-30 and 30-60 cm layer, respectively. Zhao et al. (2022) confirmed that in these fields, dissolved SIC changes to CO2, not to Ca²⁺, Mg²⁺, CO₃²⁻, or HCO₃⁻, as evidenced by the lack of SIC accumulation in deep soil, irrespective of recultivation duration, which is consistent with our findings (Fig. S1). Moreover, the authors demonstrated that the contents of Ca²⁺ and Mg²⁺, essential elements for SIC formation, remained unchanged within the top 0-90 cm, supporting the conclusion that SIC loss occurs as CO2 in these soils.

2.4.2. Mean residence time of SOC

The cumulative CO₂-OC emissions were subtracted from the initial total organic C (TOC) content of the samples to obtain the remaining SOC (%) in each sample over days of incubation. The resulting data were fitted to a double exponential decay model, but the data was best described by a single exponential decay model (Fig. S2), which follows a first order kinetics, as shown in Eq. (2):

$$A(t) = A_0 \left(e^{-kt} \right) \tag{2}$$

where, A(t) = remaining SOC (% of TOC); $A_0 = \text{main SOC pool (\% of TOC)}$; t = incubation time; $k = \text{apparent first order mineralization rate constant of SOC }(y^{-1})$.

The coefficients of determination were higher than $R^2 > 0.80$ (mostly >0.90) for all fitted models (Fig. S2). The MRT of SOC was calculated as 1/k (Derrien and Amelung, 2011).

2.4.3. Microbial biomass carbon

The microbial biomass C (MBC) content of fresh homogenized soil samples (10 g) collected from the incubation tubes at the end of incubation was determined by the chloroform fumigation-extraction method

and the MBC content was calculated using a kEC of 0.45 (Joergensen, 1996).

2.5. Density fractionation of SOM, and C and N analyses

The density fractionation was performed according to Stumpf et al. (2018). Centrifuge tubes containing 20 g of air-dried soil (weighed keeping the proportion between aggregates <2.00 mm and aggregates 8.00-2.00 mm diameter, estimated from whole soil sample, approximately 1 kg) and 80 mL of sodium polytungstate (SPT) solution (2.0 g cm⁻³) were manually shaken and thereafter centrifuged (3500 rpm, 20 min). The resulting supernatant was vacuum-filtered through a preweighted Whatman glass-microfiber filter GF/C (pore size 1-2 μm). The FLF, retained by the filter, was rinsed with 100 mL distilled water, subsequently with 50 mL CaCl₂ 0.01 M and then with another 100 mL distilled water to eliminate excess of salt (SPT). The material remaining in the tube after centrifugation was mixed again with 80 mL of SPT and this suspension was sonicated with a specific energy using an ultrasonicator processor (Vibra Cell VCX 500). The energy required for 99 % clay dispersion was determined based on exponential models relating increasing energy levels to clay content recovery. This was conducted taking into account the different soil conditions, as similarly performed by Leal et al. (2016). Recultivated soils (with 2, 4, 6 14, 30, 41 and 56 years of recultivation): 132 J mL⁻¹ (0-30 cm depth) and 140 J mL⁻¹ (30–60 cm depth); soil with 0 years of recultivation: 121 J mL⁻¹ (0–30 cm depth) and $116 \,\mathrm{J}\,\mathrm{mL}^{-1}$ (30–60 cm depth); and OS: $176 \,\mathrm{J}\,\mathrm{mL}^{-1}$ (0–30 cm layer) and 154 J mL⁻¹ (30-60 cm layer). After sonication, the dispersed suspension was centrifuged (3500 RPM, 20 min) and filtered identically to FLF. The OLF, retained by the filter, was rinsed with distilled water and CaCl2 identically as FLF. The material remaining in the tube, the heavy fraction (HF), was shaken with 150 mL distilled water, centrifuged, and the supernatant was eliminated. This procedure was repeated three times to remove excess salt (SPT) from HF. The FLF, OLF and HF fractions were oven-dried at 40 °C and weighed. The average mass recovery after fractionation was 96.1 % (0-30 cm layer) and 98.1 % (30–60 cm layer). Because the energy applied to retrieve the OLF was calculated to promote maximum aggregate dispersion, the OC and N contained in the HF remaining in the tubes are hereafter defined as mineral-associated OC (MAOC) and mineral-associated N (MAN).

The N, total C, and organic C (after removal of inorganic C by 10 % HCl treatment) content of ball-milled soil as well as of FLF and OLF samples were analyzed with an elemental analyzer (Thermo Scientific Flash 2000 coupled with a Thermo Scientific IRMS Delta V Plus, USA). The same analyzer was used to determine the isotopic signature of organic C (δ^{13} C) in the soil and SOM fractions. The MAN and MAOC content were calculated as: MAN or MAOC = [total N or OC in soil – (N or OC in FLF + OLF)].

2.6. Statistical analysis

The Shapiro-Wilk test was conducted to verify data normality and the Levene's test was performed to verify homogeneity of variances. When data normality and homogeneity of variances were confirmed, analysis of variance (ANOVA) was conducted and the means of response variables from the different sites within soil layer were compared by Tukey's test. Otherwise, the Kruskal-Wallis' test was applied and the means of response variables from the different sites within soil layer were compared by Games-Howell's test. The test applied to each response variable and soil layer is informed in the respective figures and tables. Statistical significance was set to p < 0.05. Principal component analysis (PCA) was applied to the data set to reveal shifts in the MRT of SOC and SOC stocks in FLF, OLF and MAOC, and their interrelations, over years of recultivation, at 0-30 and 0-60 cm layer. In view of the different units of MRT and SOC stocks data, the z-transformation of the data and the correlation matrix were used in PCA. The quadrants of PCA plots were named Q1, Q2, Q3 and Q4 to facilitate the interpretation of the data.

3. Results and discussion

3.1. Incomplete recovery of total SOC and MAOC stocks in the plough layer

The total SOC stock, as well as the FLF, OLF and MAOC stocks, increased significantly with recultivation years in the 0–30 cm layer, following exponential rise to maximum equations (Fig. 2). The total SOC stock increased sharply between 0 and 6 years (13.2 to 31.0 Mg C ha $^{-1}$) (Fig. 2a). About 45 % of this increase was attributed to the increase of MAOC alone, whereas 55 % was attributed to SOC increase in FLF $_{\odot}$ OLF.

The SOC stock in FLF remarkably increased between 0 and 6 years $(0.8 \text{ to } 3.9 \text{ Mg C ha}^{-1})$, i.e., before implementation of conventional agriculture (Fig. 2c). The continuous addition of plant biomass together with the addition of compost $(30-40 \text{ Mg ha}^{-1})$ to the soil during this period, are practices that are likely to explain these results (Plaza et al., 2019). For instance, the highest contribution of FLF to total SOC stocks occurred at 6 years (13 %), which was greater than that in the OS (8 %) (Fig. S3a).

The SOC stock in OLF increased from 2.1 to 8.9 Mg C ha⁻¹ between 0 and 6 years (Fig. 2e), likely favored by the combination of organic amendments (compost and plant biomass) and minimal soil disturbance within these recultivation phases (RP1, RP2), which preserve SOC occluded in aggregates and FLF as a precursor of OLF (Six et al., 2000). Here, it is important to consider that in RP1 + RP2, crop residues are eventually left on land (rather than harvested) to protect soil surface and reactivate microbial communities (Schmid et al., 2020). Furthermore, compost has been shown to promote a positive loop of soil aggregation and associated SOC storage by enhancing dissolved SOC contents, microbial biomass and formation of macroaggregates (Wang et al., 2022). Also, the residues and roots of N-fixing alfalfa, grown in the first three years of recultivation, rapidly increase soil N content and microbial activity in these soils (Reichel et al., 2017), which in turn favors aggregate formation and SOC occlusion (Veloso et al., 2020). This is associated with an exponential increase of N stocks in soil, FLF and OLF between 0 and 6 years of recultivation (Fig. 3a,c,e) and with a significant increase of MBC after 6 years of recultivation (325 mg kg⁻¹) compared to previous years (154–258 mg kg^{-1}) (Table 1).

The incorporation and occlusion of the C amendments to the soil coincide with a decline of the C:N ratio and change of the $\delta^{13} C$ in FLF and OLF after 6 years of recultivation (Table 1). Here, cementation of aggregates and SOC occlusion in early recultivated soils may be additionally favored by elevated carbonate content (40–60 Mg inorganic C ha $^{-1}$) (Fig. S1) from the loess parent material (Pilhap et al., 2019), deserving further investigation.

Conventional agriculture, which was carried out between 6 and 56 years of recultivation, reduced the rates of increase in total SOC stock (0.32 Mg C ha $^{-1}$ y $^{-1}$), and SOC in FLF (0.0001 Mg C ha $^{-1}$ y $^{-1}$) and OLF (0.14 Mg C ha $^{-1}$ y $^{-1}$) by 89 %, 100 % and 87 %, respectively, compared to the 0–6 year period. Frequent soil tillage and reduced biomass input to soil are typical of conventional agriculture and drive greater SOC mineralization rates in FLF and OLF (Six et al., 2000; Rahmati et al., 2020). After 56 years of recultivation, the SOC stocks in FLF and OLF were 3.6 and 15.8 Mg C ha $^{-1}$, respectively, and statistically equivalent to OS (Fig. 2c,e).

The MAOC stock also increased with recultivation years (Fig. 2g). However, after 56 years, the MAOC stock (27.1 Mg C ha $^{-1}$) was significantly lower by 28 % (Fig. S3c) compared to the OS (37.7 Mg C ha $^{-1}$) (Fig. 2g). Based on estimations, 129 years of the currently employed conventional agriculture system would be required to reach the MAOC stock found in OS. This agrees with a meta-analysis study showing slow recovery of SOC stocks (<0.5 Mg C ha $^{-1}$ y $^{-1}$) in degraded soils recultivated with agriculture (Baier et al., 2022). Establishment of organo-

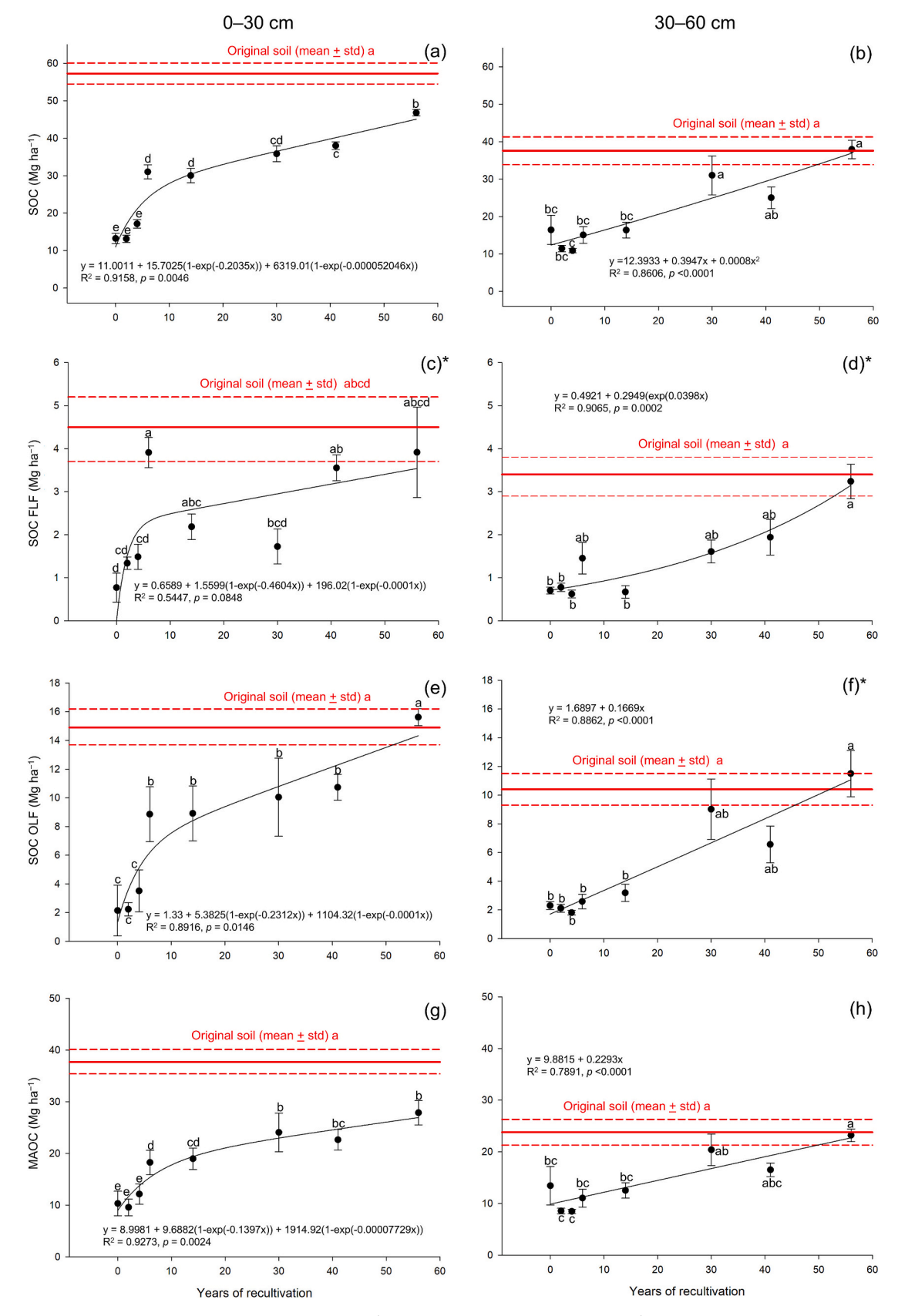


Fig. 2. Mean (n = 5) total soil organic carbon (SOC) stock (Mg C ha⁻¹) (a, b) and mean SOC stock (Mg C ha⁻¹) in free-light (FLF) (c, d), occluded-light (OLF) (e, f) and mineral-associated organic carbon (MAOC) fraction (g, h) along 56 years of soil recultivation in the 0–30 and 30–60 cm layers. Error bars are standard deviation (n = 5). Red solid and dashed lines are mean \pm standard deviation (n = 5) values of the original soil (OS). Mean values with different letters differ statistically (p < 0.05) according to Tukey's or Games-Howell's test (indicated with *).

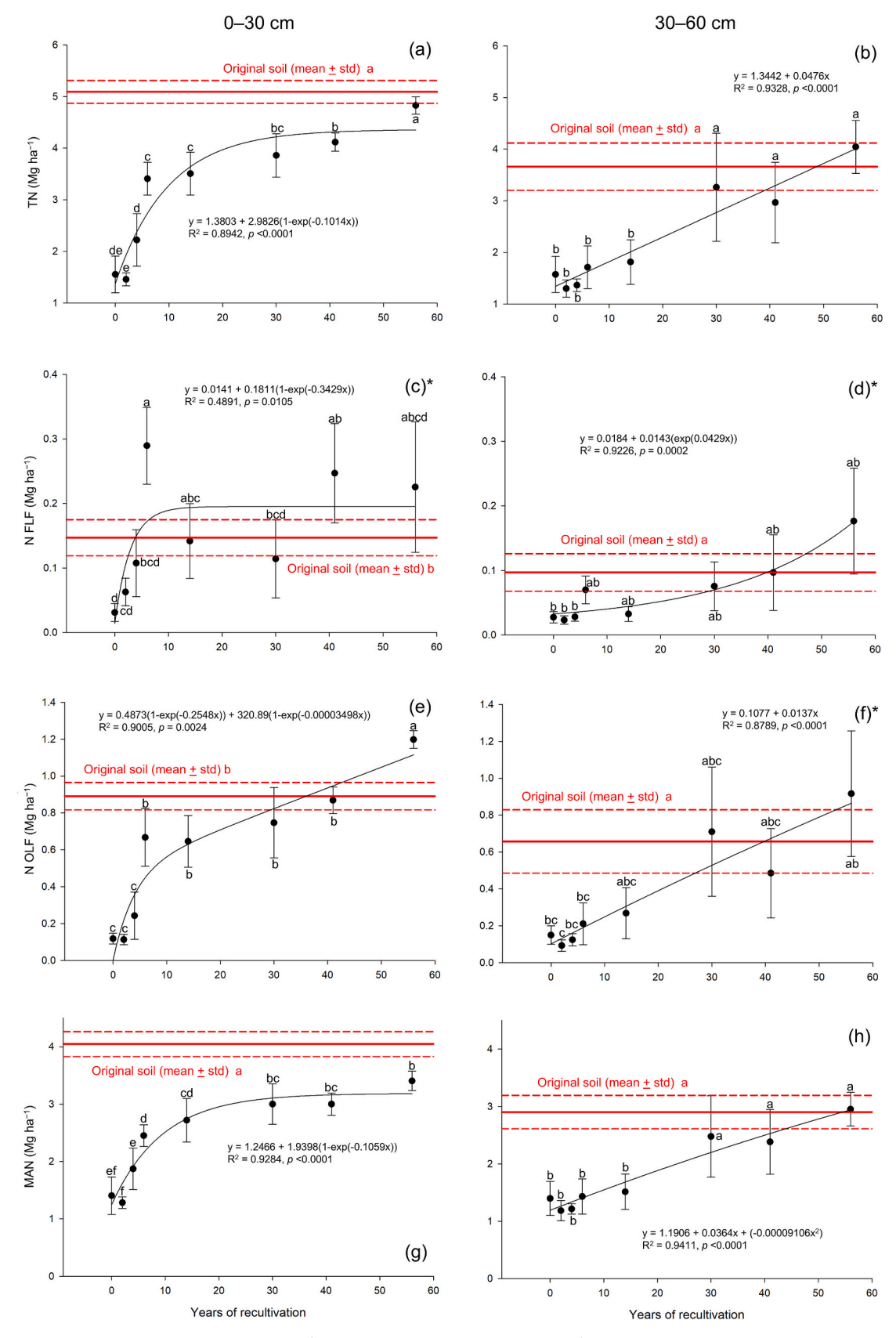


Fig. 3. Mean (n = 5) soil total nitrogen (TN) stock (Mg ha⁻¹) (a, b) and nitrogen (N) stock (Mg ha⁻¹) in the free-light (FLF) (c, d), occluded-light (OLF) (e, f) and mineral-associated N (MAN) fraction (g, h) along 56 years of soil recultivation in the 0–30 and 30–60 cm soil layers. Error bars are standard deviation (n = 5). Red solid and dashed lines are mean \pm standard deviation (n = 5) values of the original soil (OS). Mean values with different letters differ statistically (p < 0.05) according to Tukey's or Games-Howell's test (indicated with *).

Table 1 Mean and standard deviation within parentheses (n = 5) of carbon:nitrogen ratio (C:N), carbon isotopic signature (δ^{13} C) of soil and free-light (FLF), occluded-light (OLF) and mineral-associated organic carbon (MAOC) fraction, and microbial biomass carbon (MBC) content (at the end of the incubation) in the 0–30 and 30–60 cm layer across the recultivation chronosequence and at the original soil (OS).

Site	C:N				$\delta^{13}C$				MBC
	soil	FLF	OLF	MAOC	Soil	FLF	OLF	MAOC	mg kg ⁻¹
0-30	cm								
0	8.5 (0.4) c*	24.7 (6.0) ab*	18.1 (0.7) ab*	7.3 (0.4) b*	-26.2 (0.3) a	-25.5 (0.8) a	-26.1 (0.5) a*	-25.0 (0.4) a*	153.5 (25.4) d
2	9.0 (0.8) bc	22.0 (3.3) a	19.9 (1.4) a	7.4 (0.7) b	-26.4 (0.2) ab	-27.0 (0.8) bc	-26.9 (0.2) ab	-25.9 (0.2) b	208.1 (22.3) cd
4	7.8 (0.9) bc	14.1 (1.7) b	15.1 (1.8) bc	6.6 (1.2) ab	-27.4 (0.6) cd	-28.2 (0.6) c	-28.3 (0.8) bcdef	-26.7 (0.4) bcd	257.7 (23.8) bc
6	9.1 (0.4) bc	13.5 (1.1) b	13.3 (0.7) c	7.5 (0.5) b	-28.0 (0.3) e	−28.5 (0.3) c	-28.9 (0.3) ef	-27.6 (0.5) cde	324.5 (23.3) a
14	8.8 (0.3) c	14.0 (1.8) b	13.3 (0.3) c	7.3 (0.9) ab	-28.0 (0.2) e	−28.0 (0.5) c	-29.0 (0.1) f	-27.6 (0.1) e	316.2 (15.4) ab
30	9.3 (0.2) bc	15.5 (1.1) ab	13.8 (3.2) abc	8.1 (0.3) b	-26.9 (0.2) bc	-25.9 (1.1) ab	-27.7 (0.3) cd	-26.7 (0.1) c	295.0 (45.0) ab
41	9.2 (0.2) c	15.3 (3.9) ab	12.9 (0.3) c	7.7 (0.3) b	-27.7 (0.1) de	-27.9 (1.1) c	-28.6 (0.2) ef	-27.1 (0.1) d	335.0 (46.5) a
56	9.7 (0.1) b	16.7 (1.9) ab	13.2 (0.1) c	8.0 (0.4) b	-27.6 (0.2) de	−27.7 (0.3) c	-28.3 (0.2) de	-27.2 (0.1) d	325.9 (15.3) a
os	11.3 (0.3) a	31.5 (12.8) ab	16.3 (0.8) b	9.3 (0.3) a	-26.5 (0.2) ab	-25.0 (0.5) a	-27.1 (0.2) abc	−27.0 (0.1) c	312.3 (14.4) ab
30–	60 cm								
0	10.3 (4.5) ns	26.0 (3.5) b*	15.7 (1.5) ab*	7.2 (1.0) ns	-25.3 (0.7) a	-25.4 (0.3) ab	-26.8 (0.2) a*	-25.7 (0.6) abc	80.3 (17.2) b
2	8.8 (0.8)	34.5 (8.7) ab	25.2 (11.3) ab	7.3 (0.5)	-25.7 (0.2) ab	-25.6 (0.5) ab	-26.5 (0.4) a	-25.2 (0.4) a	85.5 (10.8) b
4	8.0 (0.3)	22.1 (2.7) a	14.8 (1.1) ab	7.0 (0.3)	-25.8 (0.2) ab	-26.7 (0.7) b	-26.8 (0.2) a	-25.5 (0.3) ab	79.9 (7.4) b
6	8.7 (0.9)	20.0 (7.1) ab	13.2 (2.5) ab	7.6 (1.2)	-26.4 (0.6) bcd	-26.8 (0.9) b	-27.3 (0.5) abc	-25.6 (0.5) abc	84.7 (8.7) b
14	9.0 (1.8)	20.7 (6.3) b	12.8 (4.2) ab	8.3 (1.5)	-26.9 (0.5) cd	-25.9 (0.6) ab	-28.6 (0.6) c	-26.3 (0.6) bcd	83.2 (4.4) b
30	9.4 (0.6)	23.2 (5.5) ab	12.5 (1.1) b	8.1 (0.5)	-26.8 (0.4) cd	-25.4 (0.7) ab	-27.8 (0.4) bc	-26.5 (0.4) cd	100.0 (23.2) ab
41	8.6 (1.4)	22.9 (11.5) ab	14.2 (3.0) ab	7.1 (1.4)	-26.8 (0.6) cd	-26.1 (1.2) ab	-27.7 (0.9) abc	-26.6 (0.6) d	77.9 (12.1) b
56	9.4 (0.4)	20.9 (7.7) ab	12.9 (1.5) ab	7.8 (0.3)	-27.3 (0.3) d	-26.8 (0.7) b	−28.2 (0.4) c	-26.9 (0.3) d	124.0 (25.5) a
os	10.2 (1.0)	35.1 (3.0) a	15.9 (1.3) a	8.1 (1.2)	-26.3 (0.2) abc	-24.6 (0.3) a	-26.9 (0.2) ab	-26.2 (0.2) bcd	125.9 (15.6) a

Means with different letters differ statistically (p < 0.05) according to Tukey's or Games-Howell's test (indicated with *). ns = not significant.

mineral interactions may require several decades (Lavallee et al., 2020), especially given the poor status of microbial communities found in this agricultural chronosequence (Reichel et al., 2017; Schmid et al., 2020; Roy et al., 2017, 2023). The more inefficient metabolic state of soil microorganisms to convert organic C inputs into SOC in these agricultural soils compared to its grassland counterparts has been partially attributed to imbalances between soil and microbial C:N:P stoichiometry (Clayton et al., 2021).

We also found stagnation of MAN stock after 56 years of recultivation, which was significantly lower by 16 % compared to OS (Fig. 3g), meeting our second hypothesis. Likely, this indicates a major microbial constraint to a fast and complete replenishment of MAOC stock. In a recent database analysis including over 40 studies, Manzoni and Cotrufo (2024) found that the mineral-associated SOM is predominantly fueled by necromass produced by microorganisms decomposing labile C sources and that this process is favored by microbial activity with high N demand, which results in a concomitant accrual of MAN and MAOC stocks. This has been attributed to the multifunctionality of N-containing compounds (such as phenylalanine and polypeptides/proteins), which contain additional functional groups for adsorption to mineral surfaces compared to organic compounds without N (Kleber et al., 2021). These findings align with Hu et al. (2024), who demonstrated that legume cover crops lead to greater SOC sequestration by increasing the availability of soil substrates and N stimulating microbial transformations, whereas non-legume cover cops may cause N starvation, thereby reducing microbial pathways efficiency. Apparently, the establishment of conventional agriculture on degraded soil limits the microbially driven SOC association to minerals. Since MAOC represented 59-78 % of the total SOC stocks (Fig. S3a), the slow recovery of MAOC (Fig. S3c) caused the total SOC stocks to increase at a reduced rate between 6 and 56 years of recultivation (Fig. 2g), confirming our first hypothesis. The maximum total SOC stock was reached at 56 years (46.8 Mg C ha⁻¹), when it was significantly lower by 18 % compared to OS (57.3 Mg C ha⁻¹) (Fig. 2a). Complete recovery of SOC stock relative to OS may occur only after 93 years according to our equations.

In the European Union and the United Kingdom, for example, about half of the land is used for agriculture, mainly arable land (about 110 Mha), where MAOC is particularly sensitive to loss under future climate conditions (11 % loss in RCP 8.5 scenario) (Lugato et al., 2021). Thus, it

is plausible that the slow recovery of MAOC stock observed in the plough layer in our study may stagnate or even decline before it is fully replenished, resulting in a permanent deficit of MAOC stock in this targeted layer. The linear relationship between the total SOC and MAOC stocks (Fig. 4a) indicates that the slow recovery of these stocks during recultivation years is mostly driven by the cultivation system rather than by a limited capacity of minerals to retain SOC (Cotrufo et al., 2019). For instance, assuming a maximum possible stabilization of MAOC at 82 g C kg⁻¹ silt+clay (Six et al., 2024), we estimated a MAOC stock deficit to saturation of 316.4 Mg C ha⁻¹ in this layer after 56 years of recultivation. This deficit is about 11.7 times the current MAOC stock at this sampling site, confirming that the tendency of MAOC stocks to stabilize with recultivation time likely reflects the approach of a new steady-state rather than mineral saturation, which confirms our third hypothesis. Please see calculations of MAOC deficit to saturation for both layers in the Supplemental Material.

3.2. Complete recovery of SOC stocks in the 30-60 cm layer

In the 30–60 cm layer, the total SOC stocks increased significantly from 0 to 56 years of recultivation (16.4 to $37.9 \text{ Mg C ha}^{-1}$), following a quadratic function and after 56 years did not differ statistically from OS (37.6 Mg C ha⁻¹) (Fig. 2b).

The SOC stocks in FLF increased significantly with recultivation years following an exponential growth function (Fig. 2d). The SOC stock in FLF after 56 years (3.2 Mg C $\rm ha^{-1}$) was greater than that observed after 0, 2, 4 and 14 years and did not differ statistically from OS (3.4 Mg C $\rm ha^{-1}$) (Fig. 2d). These findings indicate that the capacity of the cultivation system to introduce biomass into the subsoil was comparable to that of OS. The C:N ratio of FLF in the 30–60 cm layer in the recultivated soils (20.0–34.5) and OS (35.1) (Table 1) reflect the predominance of fresh biomass, likely root fragments, as already found below the plough layer in this chronosequence (Lucas et al., 2019) and similarly recultivated soils (Pilhap et al., 2019).

The SOC stocks in OLF increased linearly and significantly with recultivation years (Fig. 2f). The relative contribution of OLF to the total SOC stocks more than doubled from 0 (14 %) to 56 years of recultivation (30 %), reaching the level of OS (28 %) (Fig. S3b). The SOC stock in OLF after 30, 41 and 56 years (6.6–11.5 Mg C ha $^{-1}$) did not differ statistically

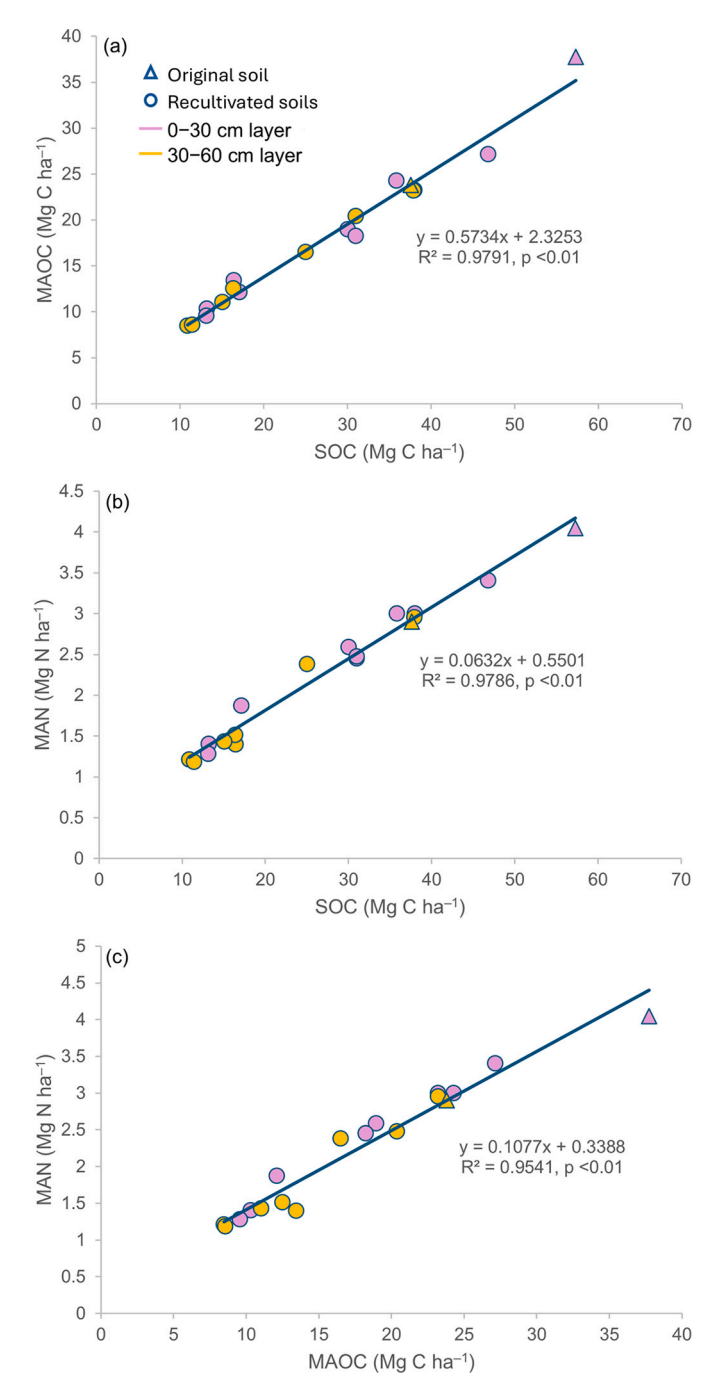


Fig. 4. Relationship between total soil organic carbon (SOC) and mineral-associated organic carbon (MAOC) stocks (a); mineral-associated nitrogen (MAN) and total SOC stocks (b); and MAN and MAOC stocks (c). Data set (n = 18) includes both 0–30 and 30–60 cm layer of recultivated and original soil.

from that in OS (10.4 Mg C ha⁻¹) (Fig. 2f). Similarly to OLF, the MAOC stocks increased linearly and significantly with recultivation years (Fig. 2h). The relative contribution of MAOC to total SOC stocks dropped from a maximum of 82 % at 0 years to a minimum of 61 % after 56 years of recultivation, which was equivalent to that in OS (63 %) (Fig. S3b). This reflects the increasing importance of FLF + OLF for SOC accrual. The MAOC stocks after 30, 41 and 56 years of recultivation (16.5–23.2 Mg C ha⁻¹) did not differ statistically between each other and from OS (23.8 Mg C ha⁻¹) (Fig. 2h). This was accompanied by a recovery of MAN stocks after 30, 41 and 56 years of recultivation (3.0–3.4 Mg C ha⁻¹), which were statistically equivalent to OS (4.0 Mg C ha⁻¹) (Fig. 3h).

The complete recovery of SOC and N stocks in FLF, OLF as well as of MAN and MAOC stocks in the 30–60 cm (Fig. 2d, f, h; Fig. 3d, f, h) layer

after 30 years coincides with the complete recovery of total SOC and N stocks in the same period (Fig. 2b; Fig. 3b). Presence of roots and absence of tillage below 30 cm depth likely favored the accumulation and occlusion of fresh SOC, as suggested by the C:N ratio of FLF (20–34.5) and OLF (12.5–25.2), which were comparable to or higher than that observed at 0–30 cm depth (Table 1). Furthermore, reduced microbial abundance and community complexity in the subsoil may spatially separate the major microbial decomposers in the topsoil from readily available C sources in the subsoil, promoting the persistence of labile SOC (Lehmann et al., 2020). For instance, the MBC content in the 30–60 cm layer (78–126 mg kg⁻¹) was lower than in the plough layer and reached that of OS (125.9 mg kg⁻¹) only after 56 years of recultivation. In contrast, in the plough layer this happened after only 6 years

(Table 1).

The replenishment of MAOC stocks at 30–60 cm may have been facilitated by the slow microbial processing of SOM derived from the topsoil and deep roots (Angst et al., 2023; Schiedung et al., 2023), and by direct association of dissolved organic C to mineral surfaces (Schiedung et al., 2023). In fact, efficient formation of MAOC in the subsoil with lower microbial abundance has been attributed to direct sorption of soluble plant and compost residues to minerals, rather than to processing of plant residues in the subsoil (Cotrufo et al., 2022).

Although the accrual of total and SOC stocks in FLF, OLF and MAOC between 0 and 56 years was greater in the 0–30 cm (33.6, 3.1, 13.7 and $16.8~{\rm Mg~C~ha}^{-1}$, respectively) than in the 30–60 cm layer (21.5, 2.5, 9.2, 9.8 Mg C ha $^{-1}$, respectively) (Table S3), we found a complete recovery of these SOC stocks relative to OS only in the 30–60 cm layer (Fig. S3). This may be also partly explained by the fact that the loss of SOC stocks in the initial recultivation soil compared to OS were larger in the 0–30 cm (loss of total SOC: 77 %, FLF: 83 %, OLF: 85 %, MAOC: 73 %) than in the 30–60 cm layer (loss of total SOC: 56 %, FLF: 80 %, OLF: 78 %, MAOC: 44 %). In absolute numbers, the loss of total SOC, FLF, OLF and MAOC in the initial recultivation soil compared to OS was 2.1-, 1.4-, 1.5 and 2.6-fold higher, respectively, in the 0–30 cm than in the 30–60 cm layer (Table S3).

3.3. Increasing MAOC stocks but decreasing MRT of SOC

In the 0–30 cm layer, the MRT of SOC decreased exponentially and significantly between 0 and 14 years of recultivation from 15.3 to 5.7 years, and thereafter increased linearly but not significantly up to 9.8 years at 56 years of recultivation (Fig. 5a). The MRT of SOC in the OS (11.7 years) differed statistically only from the MRT observed at 14 and 41 years of recultivation (MRT = 5.7 years) (Fig. 5a). In contrast, the MRT of SOC over recultivation years in the 30–60 cm layer followed an exponential decay function (Fig. 5b), and statistical differences occurred only between the MRT observed at 6 years (21.2 years) and that observed at 30 years of recultivation (8.5 years) and OS (7.7 years). Elapsed 56 years of recultivation, the MRT of SOC (9.1 years) was statistically equivalent to that in the OS (Fig. 5b).

The dynamics of the MRT of SOC observed over recultivation years in our study is mostly explained by three facts: 1) at 0 years of recultivation, MAOC contributed to 78–82 % of total SOC stocks (Fig. S3a, b) leading to relatively high MRT values (Fig. 5a, b); 2) soil recultivation

adds fresh biomass to the soil, first accumulating in FLF and OLF, which have lower MRT compared to MAOC, leading to a reduction in the MRT of SOC in the early years of recultivation; 3) the MRT values were derived from one-pool models, which best fitted the SOC loss over incubation time in our study (Fig. S2). Thus, the observed MRT values were probably modulated by a combination of natural processes leading to a decrease in MRT values due to SOC increase in FLF + OLF, which was a predominant process in early soil recultivation; and an increase in MRT values (stabilization of new SOC as MAOC), a process that became more relevant after 14 years of recultivation at 0-30 cm depth, but less so in the 30–60 cm layer. In fact, in the 0–30 cm layer the $\delta^{13}\text{C}$ of MAOC statistically and progressively decreased between 0 (-25.0 %) and 2 (-25.9 %) and between 2 and 56 (-27.2 %) years of recultivation (Table 1), likely suggesting the stabilization of new SOC. In the 30-60 cm layer, the δ^{13} C of MAOC was statistically indistinguishable between 0, 4, 6, 14 and 30 years of recultivation (variation from -25.0 to -26.5‰). Additionally, plant biomass, compost, and root-derived C input to soil and N fertilization of crops possibly promoted positive priming of MAOC (Thiessen et al., 2013; Shahbaz et al., 2017; Chari and Taylor, 2022; Tian et al., 2024), including the subsoil (Schiedung et al., 2023), ultimately preventing a more pronounced increase in MRT of SOC with recultivation age. This may be investigated in future studies. Overall, the increase in the MRT of SOC was likely hindered or masked by the limited accrual of MAOC. This is probably due to the failure of the cultivation system to promote SOC stabilization in the form of MAOC because of microbial activity demanding soil N. Our findings are in line with a reported increase in SOC stocks accompanied by reduced SOC stability after 56 years of forest restoration in highly degraded tropical soils, likely due to soil N limitation (Zhang et al., 2019).

The shift in the MRT of SOC in response to changes in SOC stocks over recultivation years is clearly illustrated in the PCA plots, where samples tend to shift from Q1 to Q2, Q3 and Q4, in this order, with recultivation years (Fig. 6). Components 1 and 2 of the PCA explained 64.1 % and 23.4 %, respectively, of the variation in the data set of the 0–30 cm layer (Fig. 6a). For the 30–60 cm layer, components 1 and 2 of PCA explained 73.6 % and 16.5 %, respectively, of the variation in the data set (Fig. 6b).

In the 0–30 cm layer, the PCA plot ordinated soils with 0, 2 and 4 years of recultivation along Q1 and Q2, which were closely associated to higher MRT values and lower SOC stocks (Fig. 6a). The plot also reveals a clear and well-ordinated shift of soils with 6, 14, 30 and 41 years of

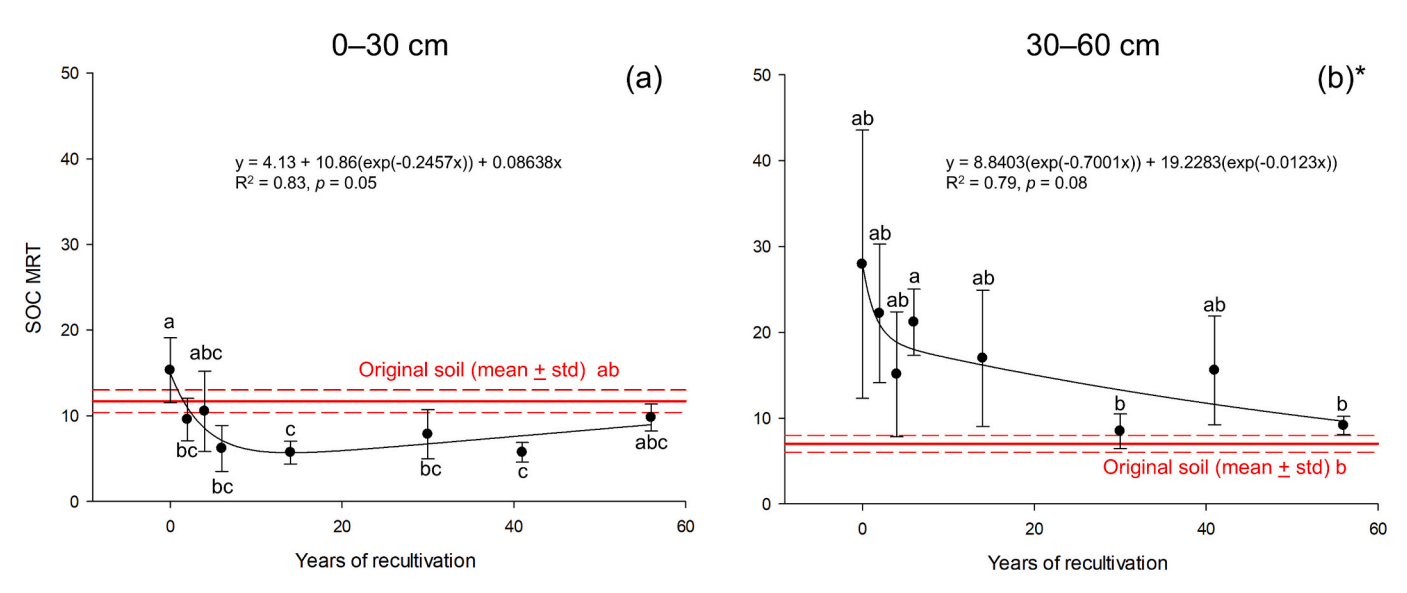
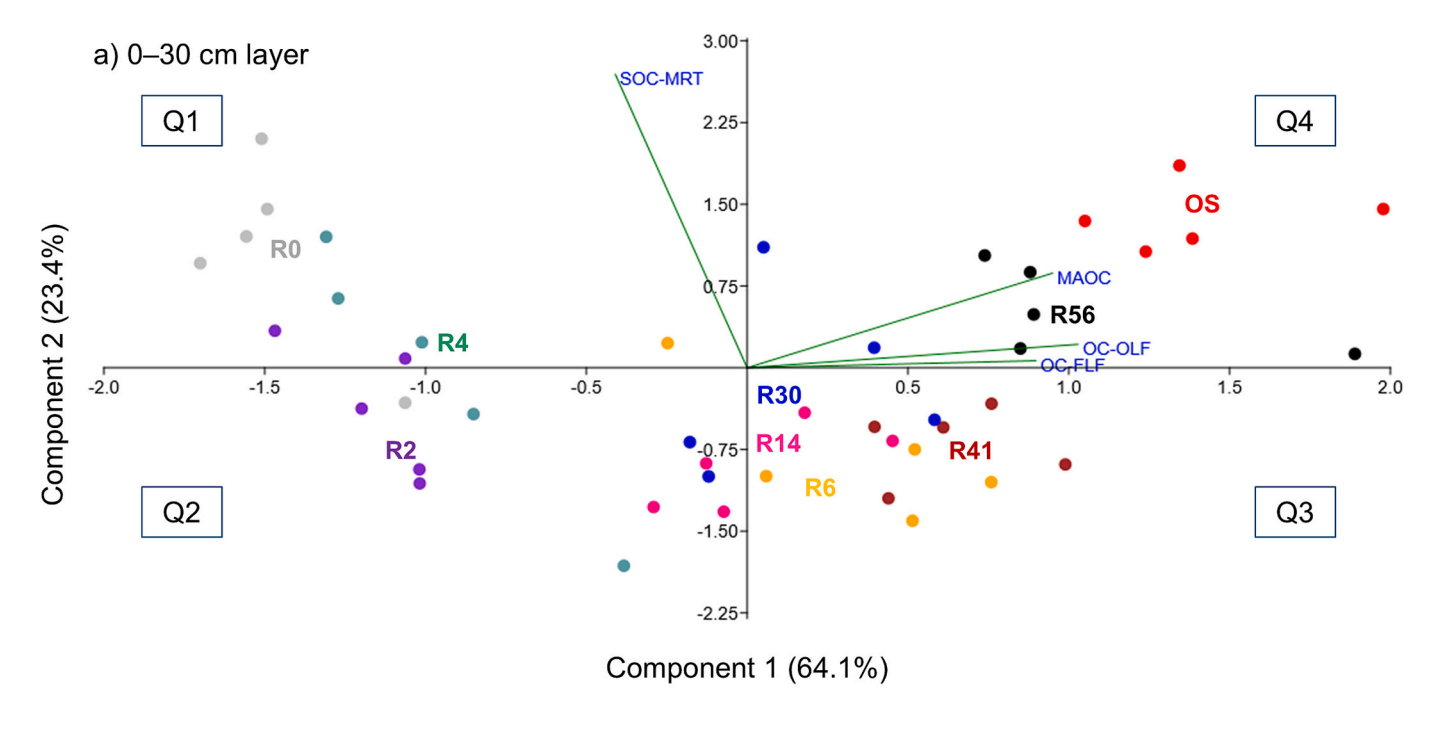


Fig. 5. Mean (n = 5) residence time (MRT) of soil organic carbon (SOC) during soil recultivation and in the original soil in the 0–30 (a) and 30–60 cm layer (b). Error bars are standard deviation (n = 5). Red solid and dashed lines are mean \pm standard deviation (n = 5) values for the MRT of SOC in OS, respectively. Mean values with different letters differ statistically (p < 0.05) according to Tukey's or Games-Howell's test (indicated with *).



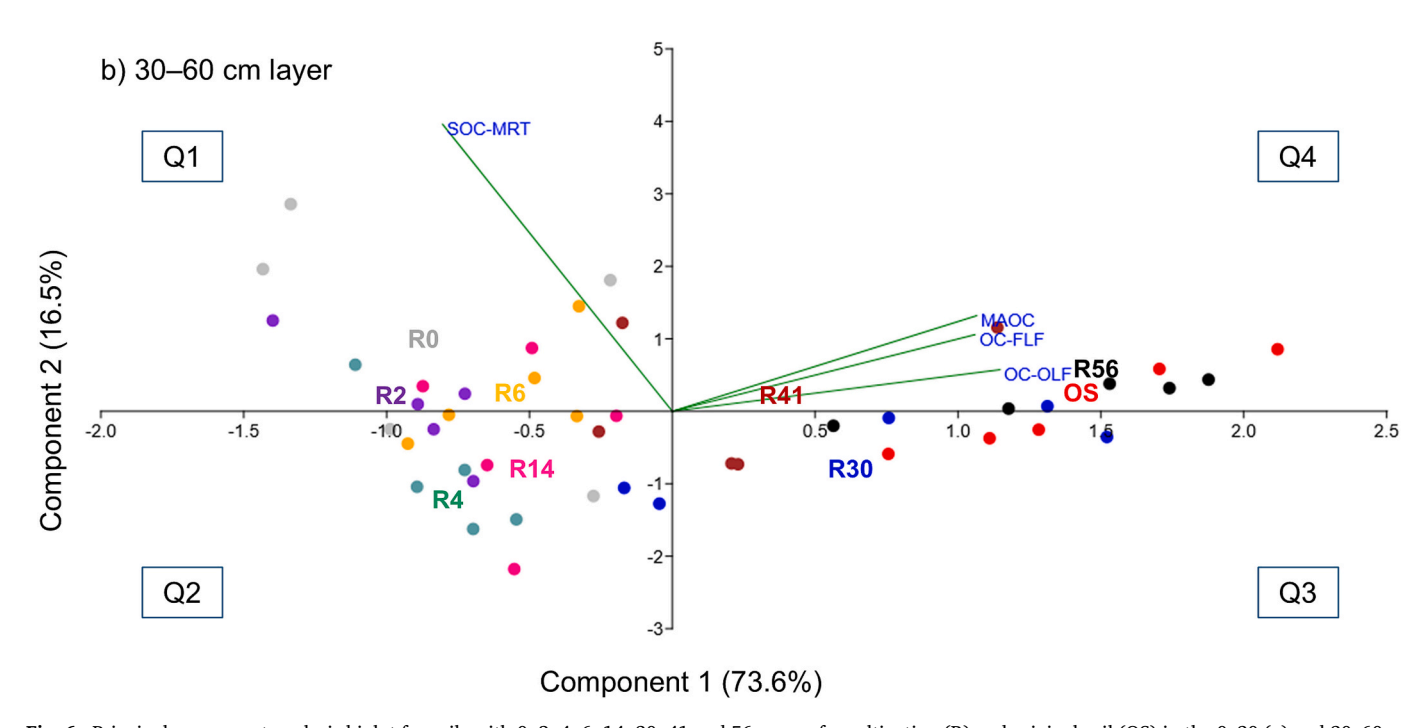


Fig. 6. Principal component analysis biplot for soils with 0, 2, 4, 6, 14, 30, 41 and 56 years of recultivation (R) and original soil (OS) in the 0–30 (a) and 30–60 cm layer (b). These group labels are centered to their five replicates and ordinated across components 1 and 2 according to their proximity to the eigenvectors indicating higher values of soil organic carbon mean residence time (SOC-MRT), and organic carbon stocks in the free-light fraction (OC-FLF), occluded-light fraction (OC-OLF) and mineral-associated organic carbon (MAOC). The labels Q1, Q2, Q3 and Q4 represent the 4 quadrants of the plot, which were used to facilitate data interpretation.

recultivation towards Q3, which is closer to FLF and OLF than to MAOC eigenvector (Fig. 6a). This confirms that the initial reduction of MRT values with years of recultivation is a response to the accrual of SOC in more labile forms (FLF + OLF) in this soil initially containing mostly MAOC. Similar interrelations between MRT values and SOC stocks are observed in the 30–60 cm layer (Fig. 6b). Nevertheless, in this layer the soils with 6 and 14 years of recultivation remained ordinated along Q1 and Q2, together with those recultivated for 0–4 years, because of their high MRT values and lower SOC stocks. A clear shift of samples towards

Q3, observed after 14 years of recultivation in 0–30 cm layer, is observed in the 30–60 cm layer only after 30 years of recultivation (Fig. 6b). This is explained by the less intense accumulation of SOC in FLF and OLF fractions in this layer compared to the upper layer. In both layers, the soil with 56 years of recultivation is plotted in Q4 together with the OS and FLF, OLF and MAOC eigenvectors (Fig. 6). However, in the 0–30 cm layer, the OS is plotted aligned with the MAOC eigenvector and further to the right in Q4 compared to the soil with 56 years of recultivation because of unreplenished MAOC stocks (Fig. 6a). In the 30–60 cm layer,

these soils are plotted closely to each other as result of their similar MRT of SOC and full replenishment of SOC stock in FLF, OLF and MAOC (Fig. 6b).

3.4. Perspectives and practices for increasing the accrual of MAOC

The linear relationship of MAN stocks with total SOC stocks (Fig. 4b) and MAOC stocks (Fig. 4c) suggests that practices enhancing N availability for microbial activity may favor the synthesis of microbial products prone to adsorption by minerals, thereby increasing MAOC stocks. This may potentially increase crop yields in this chronosequence of soils exhibiting low SOC content (0.3–1.1 %, data not shown), as indicated by a global meta-analysis reporting increase in crop yields linked to rising SOC concentrations in soils with <2 % SOC (Oldfield et al., 2019). Furthermore, these data confirm the absent saturation and the continued capacity of the minerals to accrue and stabilize SOC. For that, sufficient C and especially N must be added to soil in combination with agricultural practices favorable to SOC stabilization (Cotrufo et al., 2019; Begill et al., 2023). For instance, this was clearly evidenced in our study in the first six years of recultivation, when the highest MAOC and MAN stocks accrual rates were achieved, but this was discontinued right after conventional agriculture implementation (Fig. 2g, Fig. 3g).

The linear relationships between SOC and MAN stocks, including the OS (Fig. 4), emphasize that even the SOC stocks of the OS can be increased by targeting agricultural practices that favor long-term SOC stabilization, as conceptualized in Fig. 7. This is supported by the large MAOC stock deficit to saturation estimated for the OS at 0–30 cm (296.5 Mg ha⁻¹) and 30–60 cm (301.0 Mg ha⁻¹) layer (calculations presented in Supplemental Material). These practices usually include reduced tillage, soil cover by biomass, consistent and increased biomass input to soil (especially N-rich biomass), organic amendments (e.g., compost, manure), crop diversification and legume cover crops, among others (Veloso et al., 2018; Zanatta et al., 2019; Lehmann et al., 2020; Pol et al., 2022; King et al., 2024). Such practices can be adapted to local management and climatic conditions, also to offset additional MAOC losses caused by climate warming (Amelung et al., 2020; Riggers et al., 2021).

For instance, current research emphasizes that to reach the target stablished by global initiatives to increase SOM by 4 ‰ y^{-1} within the top 30 cm of mineral agricultural soils the C inputs to soil have to be largely increased, especially in Northern and Central Europe respectively by 1.85 and 1.20 Mg C ha $^{-1}$ yr $^{-1}$ under RCP 2.6 and by 2.60 and 2.21 Mg C ha $^{-1}$ yr $^{-1}$ under RCP 6, and that agricultural practices driving SOC stabilization have to be prioritized (Bruni et al., 2024). This meets the European Climate Law which provides for the European Union to become climate neutral by 2050 (European Commission, 2022a) and the Nature Restoration Law of the European Union which sets the goal that 100 % of the European Union's degraded land should be covered by restoration measures by 2050. Increasing SOC stocks in the top 30 cm of mineral agricultural soils is assumed as a central strategy to meet this obligation (European Commission, 2022b).

4. Conclusions

Our study highlighted the lower stock of stabilized SOC in the recultivated soils compared to the original soil in the plough layer. This was assigned to the legacy of severe soil degradation coupled with the limited capacity of the cultivation system to promote continued accrual of MAOC, rather than to limited capacity of minerals to stabilize SOC. We found that conventional agriculture establishment on these severely degraded soils may unlikely restore total SOC and MAOC stocks in the plough layer to the original conditions before 93 and 129 years, respectively. In a critical climate-change scenario, these stocks may even stagnate or decline before they are fully replenished. Moreover, direct implementation of conventional agriculture on highly degraded soils without minimal soil preconditioning such as legume cultivation (alfalfa) and low soil disturbance in the first recultivation phases (as performed in the studied chronosequence) may dampen the recovery of MAOC stocks observed here.

We revealed that simply the long duration of recultivation of degraded soils with conventional agriculture may not resolve N as a limiting factor for microbially driven SOC stabilization. Our findings strongly converged with state-of-art literature studying mechanisms of

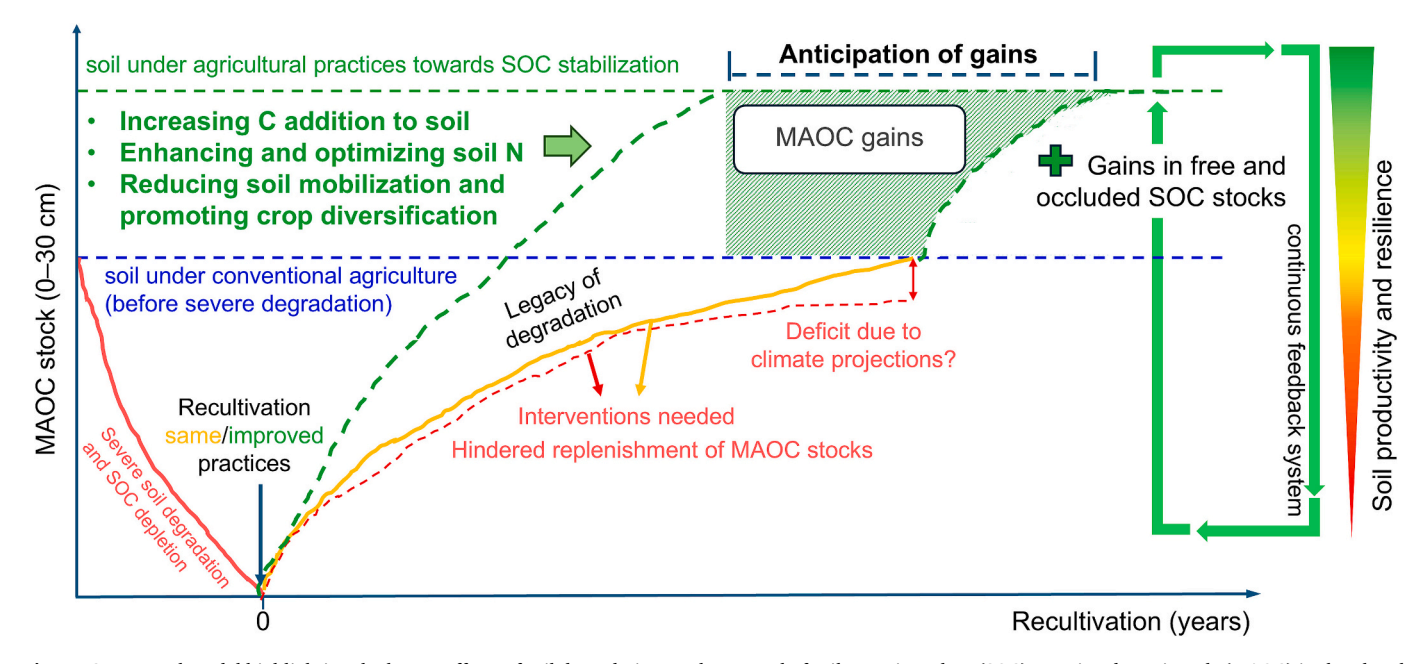


Fig. 7. Conceptual model highlighting the legacy effects of soil degradation on the accrual of soil organic carbon (SOC) associated to minerals (MAOC) in the plough layer (0–30 cm) when conventional agricultural practices are continuously applied to recultivate severely degraded soils. The model outlines key practices to enhance MAOC accrual rates, as 1) increasing C addition to soil: supports the buildup of free, occluded and mineral-associated SOC stocks; 2) enhancing and optimizing soil N levels: crucial for promoting microbial activity driving MAOC accrual; and 3) reducing soil mobilization and promoting crop diversification: together with the previous practices this optimizes C and N entering the soil and creates a continuous feedback mechanisms to enhance soil productivity and resilience and to sustain the system in the long-term.

SOC stabilization associated with soil N use by microorganisms. Therefore, recultivation practices to promote long-term SOC stabilization should be prioritized continuously since early stages of soil recultivation aiming to replenish or ideally gain additional MAOC stocks. Furthermore, we demonstrated that such practices may likely enhance the MAOC stocks of the original soil as well (not disturbed by mining).

CRediT authorship contribution statement

Otávio dos Anjos Leal: Visualization, Methodology, Investigation, Formal analysis, Data curation, Conceptualization, Writing – review & editing, Writing – original draft. Rüdiger Reichel: Investigation, Formal analysis, Data curation, Writing – review & editing, Writing – original draft. Holger Wissel: Methodology, Formal analysis, Data curation. Nicolas Brüggemann: Supervision, Resources, Project administration, Methodology, Investigation, Funding acquisition, Conceptualization, Writing – review & editing, Writing – original draft.

Declaration of competing interest

The authors declare that they have no known competing financial interests or personal relationships that could have appeared to influence the work reported in this paper.

Acknowledgments

We are particularly grateful to Manuel Endenich (RWE Power AG, Germany) for information on the reclamation process and access to the sampling sites, and to Sirgit Kummer for assistance in the determination of soil microbial biomass carbon. We would also like to thank the German Federal Ministry of Education and Research (BMBF) for funding the INPLAMINT project under the BonaRes initiative (031B1062A, Nicolas Brüggemann). The first author thanks the Alexander von Humboldt Foundation for a Renewed Research Stay grant.

Appendix A. Supplementary data

Supplementary data to this article can be found online at $\frac{\text{https:}}{\text{doi.}}$ org/10.1016/j.scitotenv.2025.179445.

Data availability

Data will be made available on request.

References

- Amelung, W., Bossio, D., de Vries, W., Kögel-Knabner, I., Lehmann, J., Amundson, R., Bol, R., Collins, C., Lal, R., Leifeld, J., Minasny, B., Pan, G., Paustian, K., Rumpel, C., Sanderman, J., van Groenigen, J.W., Mooney, S., van Wesemael, B., Wander, M., Chabbi, A., 2020. Towards a global-scale soil climate mitigation strategy. Nat. Commun. 11, 1. https://doi.org/10.1038/s41467-020-18887-7.
- Angst, G., Mueller, K.E., Castellano, M.J., Vogel, C., Wiesmeier, M., Mueller, C.W., 2023. Unlocking complex soil systems as carbon sinks: multi-pool management as the key. Nat. Commun. 14, 2967. https://doi.org/10.1038/s41467-023-38700-5.
- Baier, C., Modersohn, A., Jalowy, F., Glaser, B., Gross, A., 2022. Effects of recultivation on soil organic carbon sequestration in abandoned coal mining sites: a meta-analysis. Sci. Rep. 12, 20090. https://doi.org/10.1038/s41598-022-22937-z.
- Begill, N., Don, A., Poeplau, C., 2023. No detectable upper limit of mineral-associated organic carbon in temperate agricultural soils. Glob. Change Biol. 29, 4662–4669. https://doi.org/10.1111/gcb.16804.
- Bruni, E., Lugato, E., Chenu, C., Guenet, B., 2024. European croplands under climate change: carbon input changes required to increase projected soil organic carbon stocks. Sci. Total Environ. 954, 176525. https://doi.org/10.1016/j.scitotenv.2024.176525.
- Castro-Herrera, D., Prost, K., Kim, D.-G., Yimer, F., Tadesse, M., Gebrehiwot, M., Brüggemann, N., 2023. Biochar addition reduces non-CO₂ greenhouse gas emissions during composting of human excreta and cattle manure. J. Environ. Qual. 52 (4), 814–828. https://doi.org/10.1002/jeq2.20482.
- Chari, N.R., Taylor, B.N., 2022. Soil organic matter formation and loss are mediated by root exudates in a temperate forest. Nat. Geosci. 15, 1011–1016. https://doi.org/ 10.1038/s41561-022-01079-x.

- Clayton, J., Lemanski, K., Bonkowski, M., 2021. Shifts in soil microbial stoichiometry and metabolic quotient provide evidence for a critical tipping point at 1% soil organic carbon in an agricultural post-mining chronosequence. Biol. Fert. Soils 57, 435–446. https://doi.org/10.1007/s00374-020-01532-2.
- Cotrufo, M.F., Lavalle, J.M., 2022. Soil organic matter formation, persistence, and functioning: a synthesis of current understanding to inform its conservation and regeneration. Adv. Agron. 172, 1–66. https://doi.org/10.1016/bs.agron.2021.11.002.
- Cotrufo, M.F., Ranalli, M.G., Haddix, M.L., Six, J., Lugato, E., 2019. Soil carbon storage informed by particulate and mineral-associated organic matter. Nat. Geosci. 12, 898–994. https://doi.org/10.1038/s41561-019-0484-6.
- Cotrufo, M.F., Haddix, M.L., Kroeger, M.E., Stewart, C.E., 2022. The role of plant input physical-chemical properties, and microbial and soil chemical diversity on the formation of particulate and mineral-associated organic matter. Soil Biol. Biochem. 168, 108648. https://doi.org/10.1016/j.soilbio.2022.108648.
- Creamer, C.A., Filley, T.R., Boutton, T.W., 2013. Long-term incubations of size and density separated soil fractions to inform soil organic carbon decay dynamics. Soil Biol. Biochem. 57, 496e503. https://doi.org/10.1016/j.soilbio.2012.09.007.
- Crow, S.E., Sulzman, E.W., Rugh, W.D., Bowden, R.D., Laitha, K., 2006. Isotopic analysis of respired CO2 during decomposition of separated soil organic matter pools. Soil Biol. Biochem. 38, 3279–3291. https://doi.org/10.1016/j.soilbio.2006.04.007.
- Derrien, D., Amelung, W., 2011. Computing the mean residence time of soil carbon fractions using stable isotopes: impacts of the model framework. Eur. J. Soil Sci. 62, 237–252. https://doi.org/10.1111/j.1365-2389.2010.01333.x.
- Dworschak, U., Rose, U., 2014. Das Rheinische Braunkohlenrevier. In: Handbuch Naturschutz und Landschaftspflege. Wiley and Sons, New York, pp. 1–23.
- European Commission, 2021. Communication from the commission to the European parliament, the council, the European economic and social committee and the committee of the regions. In: EU Soil Strategy for 2030. Reaping the Benefits of Healthy Soils for People, Food, Nature and Climate SWD(2021) 323 Final. COM (2021) 699 Final.
- European Commission, 2022a. Proposal for a regulation of the European Parliament and of the council establishing a union certification framework for carbon removals {SEC (2022) 423 final} {SWD(2022) 377 final} {SWD(2022) 378 final}. In: COM(2022) 672 final, 2022/0394 (COD).
- European Commission, 2022b. Proposal for a regulation of the European Parliament and of the council on nature restoration. In: COM(2022) 304 final, 2022/0195(COD).
- FAO, 2022. Global Symposium on Soil Erosion. https://www.fao.org/about/meetings/soil-erosion-symposium/key-messages/en/ (accessed 09 February 2024).
- Georgiou, K., Jackson, R.B., Vindušková, O., Abramoff, R.Z., Ahlström, Á., Feng, W., Harden, J.W., Pellegrini, A.F.A., Polley, H.W., Soong, J.L., Riley, W.J., Torn, M.S., 2022. Global stocks and capacity of mineral-associated soil organic carbon. Nat. Commun. 13, 3797. https://doi.org/10.1038/s41467-022-31540-9.
- Haddix, M.L., Greogorich, E.G., Helgason, B.L., Janzen, H., Ellert, B.H., Cotrufo, M.F., 2020. Climate, carbon content, and soil texture control the independent formation and persistence of particulate and mineral-associated organic matter in soil. Geoderma 363, 114160. https://doi.org/10.1016/j.geoderma.2019.114160.
- Hansen, P.M., Even, R., King, A.E., Lavallee, J., Schipanski, M., Cotrufo, M.F., 2024. Distinct, direct and climate-mediated environmental controls on global particulate and mineral-associated organic carbon storage. Glob. Change Biol. 30, e17080. https://doi.org/10.1111/gcb.17080.
- Hu, Q., Zhang, Y., Cao, W., Yang, Y., Hu, Y., He, T., Li, Z., Wang, P., Chen, X., Chen, J., Shi, X., 2024. Legume cover crops sequester more soil organic carbon than nonlegume cover crops by stimulating microbial transformations. Geoderma, 117024. https://doi.org/10.1016/j.geoderma.2024.117024.
- IUSS Working Group WRB, 2015. World reference base for soil resources 2014. Update 2015. In: World Soil Resource Reports, 106. FAO, Rome.
- Jobbágy, E.G., Jackson, R.B., 2000. The vertical distribution of soil organic carbon and its relation to climate and vegetation. Ecol. Appl. 10 (2), 423–436. https://doi.org/ 10.1890/1051-0761(2000)010[0423:TVDOS0]2.0.CO;2.
- Joergensen, R.G., 1996. The fumigation-extraction method to estimate soil microbial biomass. Calibration of the k_{EC} value. Soil Biol. Biochem. 28, 25–31. https://doi.org/ 10.1016/0038-0717(95)00102-6.
- King, A.E., Amsili, J.P., Córdova, S.C., Culman, S., Fonte, S.J., Kotcon, J., Masters, M.D., McVay, K., Olk, D.C., Prairie, A.M., Schipanski, M., Schneider, S.K., Stewart, C.E., Cotrufo, M.F., 2024. Constraints on mineral-associated and particulate organic carbon response to regenerative management: carbon inputs and saturation deficit. Soil Till. Res. 238, 106008. https://doi.org/10.1016/j.still.2024.106008.
- Kleber, M., Eusterheus, K., Keiluweit, M., Mikutta, C., Mikutta, R., Nico, P.S., 2015. Mineral–organic associations: formation, properties, and relevance in soil environments. Adv. Agron. 130, 1–140. https://doi.org/10.1016/bs. agron.2014.10.005.
- Kleber, M., Bourg, I.C., Coward, E.K., Hansel, C.M., Myneni, S.C.B., Nunan, N., 2021. Dynamic interactions at the mineral-organic matter interface. Nat. Rev. Earth. Environ. 2, 402–421. https://doi.org/10.1038/s43017-021-00162-y.
- Knicker, H., González-Vila, F.J., González-Vázquez, R., 2013. Biodegradability of organic matter in fire-affected mineral soils of southern Spain. Soil Biol. Biochem. 56, 31–39. https://doi.org/10.1016/j.soilbio.2012.02.021.
- Landesoberbergamt, N., 1986. Richtlinien des Landesoberbergamt Nordrhein-Westfalen für das Aufbringen von kulturfähigem Bodenmaterial bei landwirtschaftlicher Rekultivierung für die im Tagebau betriebenen Braunkohlenwerke vom 22.7.1986. Sammelblatt des Landesoberbergamtes Nordrhein-Westfalen A2, 29.
- Lavallee, J.M., Soong, J.L., Cotrufo, M.F., 2020. Conceptualizing soil organic matter into particulate and mineral-associated forms to address global change in the 21st century. Glob. Change Biol. 26, 261–273. https://doi.org/10.1111/gcb.14859.

- Leal, O.A., Castilhos, R.M.V., Pinto, L.F.S., Pauletto, E.A., Lemes, E.S., Kunde, R.J., 2016. Initial recovery of organic matter of a grass-covered constructed soil after coal mining. Rev. Bras. Cienc. Solo. 40, 0150384. https://doi.org/10.1590/ 18069657rbcs20150384.
- Lehmann, J., Hansel, C.M., Kaiser, C., Kleber, M., Maher, K., Manzoni, S., Nunan, N., Reichstein, M., Schimel, J.P., Torn, M.S., Wieder, W.R., Kögel-Knabner, I., 2020. Persistence of soil organic carbon caused by functional complexity. Nat. Geosci. 13, 529–534. https://doi.org/10.1038/s41561-020-0612-3.
- Lössabkommen, N., 1961. Einigung über die Lößschütthöhe auf den landwirtschaftlich zur rekultivierenden Flächen im Bereich der bereits beendeten und der zurzeit beriebenen Tagebaue der der Rheinischen Braunkohlen AG einschließlich deren Außenkippen zwischen dem min. f. Wirtschaft, Mittelstand und Verkehr, dem Min. f. Ernährung, Landwirtschaft und Forsten, der Landesplanungsbehörde und der Rheinischen Braunkohlen AG vom 20.2.1961.
- Lucas, M., Schlüter, S., Vogel, H., Vetterlein, D., 2019. Soil structure formation along an agricultural chronosequence. Geoderma 350, 61–72. https://doi.org/10.1016/j. geoderma.2019.04.041.
- Lugato, E., Lavallee, J.M., Haddix, M.L., Panagos, P., Cotrufo, M.F., 2021. Different climate sensitivity of particulate and mineral-associated soil organic matter. Nat. Geosci. 14, 295–300. https://doi.org/10.1038/s41561-021-00744-x.
- Maaßen, U., Schiffer, H.-W., 2019. The German Lignite Industry in 2018. World of Mining – Surface & Underground.
- Machmuller, M.B., Kramer, M.G., Cyle, T.K., Hill, N., Hancock, D., Thompson, A., 2015.
 Emerging land use practices rapidly increase soil organic matter. Nat. Commun. 6, 6995. https://doi.org/10.1038/ncomms7995.
- Manzoni, S., Cotrufo, F., 2024. Mechanisms of soil organic carbon and nitrogen stabilization in mineral associated organic matter – insights from modelling in phase space. Biogeosciences 21, 4077–4098. https://doi.org/10.5194/egusphere-2024-1092
- Mao, H.-R., Cotrufo, M.F., Hart, S.C., Sullivan, B.W., Zhu, X., Zhang, J., Liang, C., Zhu, M., 2024. Dual role of silt and clay in the formation and accrual of stabilized soil organic carbon. Soil Biol. Biochem. 192, 109390. https://doi.org/10.1016/j. spilbic.2024.109300
- Matos, E.S., Freese, D., Böhm, C., Quinkenstein, A., Hüttl, R., 2012. Organic matter dynamics in reclaimed lignite mine soils under *Robinia pseudoacacia* L. plantations of different ages in Germany. Commun. Soil Scie. Plant Anal. 43, 5, 745–755. https:// doi.org/10.1080/00103624.2012.648354.
- Öhlinger, R., 1996. Maximum water-holding capacity. In: Methods in Soil Biology. Springer, Heidelberg, Germany.
- Oldfield, E.E., Bradford, M.A., Wood, S.A., 2019. Global meta-analysis of the relationship between soil organic matter and crop yields. Soil 5, 15–32. https://doi.org/10.5194/ soil-5-15-2019.
- Padarian, J., Stockmann, U., Minasny, B., McBratney, A.B., 2022. Monitoring changes in global soil organic carbon stocks from space. Remote Sens. Environ. 281, 113260. https://doi.org/10.1016/j.rse.2022.113260.
- Paul, S., Flessa, H., Veldkamp, E., López-Ulloa, M., 2008. Stabilization of recent soil carbon in the humid tropics following land use changes: evidence from aggregate fractionation and stable isotope analyses. Biogeochemistry 87, 247–263. https://doi. org/10.1007/s10533-008-9182-y.
- Pilhap, E., Vuko, M., Lucas, M., Steffens, M., Schloter, M., Vetterlein, D., Endenich, M., Kögel-Knabner, I., 2019. Initial soil formation in an agriculturally reclaimed opencast mining area - the role of management and loess parent material. Soil Till. Res. 191, 224–237. https://doi.org/10.1016/j.still.2019.03.023.
- Plaza, C., Giannetta, B., Benavente, I., Vischetti, C., Zaccone, C., 2019. Density-based fractionation of soil organic matter: effects of heavy liquid and heavy fraction washing. Sci. Rep. 9, 10146. https://doi.org/10.1038/s41598-019-46577-y.
- Poeplau, C., Jacobs, A., Don, A., Vos, C., Schneider, F., Wittnebel, M., Tiemeyer, B., Heidkamp, A., Prietz, R., Flessa, H., 2020. Stocks of organic carbon in German agricultural soils—key results of the first comprehensive inventory. J. Plant Nutr. Soil Sc. 183, 665–681. https://doi.org/10.1002/jpln.202000113.
- Poeplau, C., Don, A., Schneider, F., 2021. Roots are key to increasing the mean residence time of organic carbon entering temperate agricultural soils. Glob. Change Biol. 27, 4921–4934. https://doi.org/10.1111/gcb.15787.
- Pol, L.K., Robertson, A., Schipanski, M., Calderon, F.J., Wallenstein, M.D., Cotrufo, M.F., 2022. Addressing the soil carbon dilemma: legumes in intensified rotations regenerate soil carbon while maintaining yields in semi-arid dryland wheat farms. Agr. Ecosyst. Environ. 330, 107906. https://doi.org/10.1016/j.agee.2022.107906.
- Rahmati, M., Eskandari, I., Kouselou, M., Feiziasl, V., Mahdavinia, N., McKenzie, B.M., 2020. Changes in soil organic carbon fractions and residence time five years after implementing conventional and conservation tillage practices. Soil Till. Res. 200, 104632. https://doi.org/10.1016/j.still.2020.104632.
- Reichel, R., Hänsch, M., Brüggemann, N., 2017. Indication of rapid soil food web recovery by nematode-derived indices in restored agricultural soil after open-cast lignite mining. Soil Biol. Biochem. 115, 261–264. https://doi.org/10.1016/j. soilbio.2017.08.020.
- Reichel, R., Hänsch, M., Schulz, S., Martins, B.R., Schloter, M., Brüggemann, N., 2024. Comparing a real and pseudo chronosequence of mining soil reclamation using freeliving nematodes to characterize the food web and C and N dynamics. Agr. Ecosyst. Environ. 376, 109234. https://doi.org/10.1016/j.agee.2024.109234.

- Riggers, C., Poeplau, C., Don, A., Frühauf, C., Dechow, R., 2021. How much carbon input is required to preserve or increase projected soil organic carbon stocks in German croplands under climate change? Plant and Soil 460, 417–433. https://doi.org/ 10.1007/s11104-020-04806-8.
- Roy, J., Reichel, R., Brüggemann, N., Hempel, S., Rillig, M.C., 2017. Succession of arbuscular mycorrhizal fungi along a 52-year agricultural recultivation chronosequence. FEMS Microbiol. Ecol. 93, fix102. https://doi.org/10.1093/ femsec/fix102
- Roy, J., Reichel, R., Brüggemann, N., Rillig, M.C., 2023. Functional, not taxonomic, composition of soil fungi reestablishes to pre-mining initial state after 52 years of recultivation. Microb. Ecol. 86, 213–223. https://doi.org/10.1007/s00248-022-02058-w
- Sandermann, J., Hengl, T., Fiske, G.J., 2017. Soil carbon debt of 12,000 years of human land use. PNAS 114, 36, 9575–9580. https://doi.org/10.1073/pnas.1706103114.
- Schiedung, M., Don, A., Beare, M.H., Abiven, S., 2023. Soil carbon losses due to priming moderated by adaptation and legacy effects. Nat. Geosci. 16, 909–914. https://doi. org/10.1038/s41561-023-01275-3.
- Schmid, C.A.O., Reichel, R., Schröder, P., Brüggemann, N., Schloter, M., 2020. 52 years of ecological restoration following a major disturbance by opencast lignite mining does not reassemble microbiome structures of the original arable soils. Sci. Total Environ. 745, 140955. https://doi.org/10.1016/j.scitotenv.2020.140955.
- Schmidt, M.W.I., Torn, M., Abiven, S., Dittmar, T., Guggenberger, G., Jansses, I.A., Kleber, M., Kögel-Knabner, I., Lehmann, J., Manning, D.A.C., Nannipieri, P., Rasse, D.P., Weiner, S., Trumbore, S.E., 2011. Persistence of soil organic matter as an ecosystem property. Nature 478, 49–56. https://doi.org/10.1038/nature10386.
- Shahbaz, M., Kuzyakov, Y., Heitkamp, F., 2017. Decrease of soil organic matter stabilization with increasing inputs: mechanisms and controls. Geoderma 304, 76–82. https://doi.org/10.1016/j.geoderma.2016.05.019.
- Six, J., Elliott, E.T., Paustian, K., 2000. Soil macroaggregate turnover and microaggregate formation: a mechanism for C sequestration under no-tillage agriculture. Soil Biol. Biochem. 32, 2099–2103. https://doi.org/10.1016/S0038-0717(00)00179-6.
- Six, J., Doertterl, S., Laub, M., Müller, C.R., Van de Broek, M., 2024. The six rights of how and when to test for soil C saturation. SOIL 10, 275–279. https://doi.org/10.5194/soil-10-275-2024.
- Stockmann, U., et al., 2013. The knowns, known unknowns and unknowns of sequestration of soil organic carbon. Agr. Ecosyst. Environ. 164, 80–99. https://doi. org/10.1016/j.agee.2012.10.001.
- Stumpf, L., Leal, O.A., Pauletto, E.A., Pinto, L.F.S., Reis, D.A., Pinto, M.A.B., Tuchtenhagen, I.K., 2018. Tensile strength and organic matter fractions in aggregates of a grass-covered mined soil under early stage recovery. Soil Till. Res. 176, 69–76. https://doi.org/10.1016/j.istill.2017.11.006.
- Thiessen, S., Gleixner, G., Wutzler, T., Reichstein, M., 2013. Both priming and temperature sensitivity of soil organic matter decomposition depend on microbial biomass e an incubation study. Soil Biol. Biochem. 57, 739–748. https://doi.org/ 10.1016/i.soilbio.2012.10.029.
- Tian, J., Dungait, J.A.J., Hou, R., Deng, Y., Hartley, I.P., Yang, Y., Kuzyakov, Y., Zhang, F., Cotrufo, M.F., Zhou, J., 2024. Microbially mediated mechanisms underlie soil carbon accrual by conservation agriculture under decade-long warming. Nat. Commun. 15, 377. https://doi.org/10.1038/s41467-023-44647-4.
- VDLUFA, 1991. Method book I. Determination of the gravimetric water content (A 2.1.1). Determination of the soil PH in CaCl₂ extracts (a 5.1.1). In: Determination of Mineral N (Nmin: NO₃ and NH₄) in Soil Profiles (A 6.1.4.1). Association of German Agricultural Analytic and Research Institutes, VDLUFA-Verlag, Germany. Veloso, M.G., Angers, D.A., Tiecher, T., Giacomini, S., Dieckow, J., Bayer, C., 2018. High
- Veloso, M.G., Angers, D.A., Tiecher, T., Giacomini, S., Dieckow, J., Bayer, C., 2018. High carbon storage in a previously degraded subtropical soil under no-tillage with legume cover crops. Agric. Ecosyst. Environ. 268, 15–23. https://doi.org/10.1016/j. agee.2018.08.024.
- Veloso, M.G., Angers, D.A., Chantigny, M.H., Bayer, C., 2020. Carbon accumulation and aggregation are mediated by fungi in subtropical soil under conservation agriculture. Geoderma 363, 114159. https://doi.org/10.1016/j.geoderma.2019.114159.
- Wang, D., Lin, J.Y., Sayre, J.M., Schmidt, R., Fonte, S.J., Rodrigues, J.J.L.M., Scow, K.M., 2022. Compost amendment maintains soil structure and carbon storage by increasing available carbon and microbial biomass in agricultural soil – a six-year field study. Geoderma 427, 116117. https://doi.org/10.1016/j. geoderma.2022.116117.
- Zanatta, J.A., Vieira, F.C.B., Biedis, C., Dieckow, J., Bayer, C., 2019. Carbon indices to assess quality of management systems in a subtropical acrisol. Sci. Agric. 76 (6), 501–508. https://doi.org/10.1590/1678-992X-2017-0322.
- Zhang, H., Deng, Q., Hui, D., Wu, J., Xiong, X., Zhao, J., Zhao, M., Chu, G., Zhou, G., Zhang, D., 2019. Recovery in soil carbon stock but reduction in carbon stabilization after 56-year forest restoration in degraded tropical lands. Forest Ecol. Manag. 441, 1–8. https://doi.org/10.1016/j.foreco.2019.03.037.
- Zhao, Y., Reichel, R., Herbst, M., Sun, Y., Brüggemann, N., Mörchen, R., Welp, G., Meng, F., Bol, R., 2022. Declining total carbon stocks in carbonate-containing agricultural soils over a 62-year recultivation chronosequence under humid conditions. Geoderma 425, 116060. https://doi.org/10.1016/j.geoderma.2022.116060.